Journal of Hydrology 653 (2025) 132775

Contents lists available at ScienceDirect

Journal of Hydrology

journal homepage: www.elsevier.com/locate/jhydrol

Research papers

A chloride threshold to identify the onset of seawater/saltwater intrusion and a novel categorization of groundwater in coastal aquifers

M.D. Fidelibus [a], G. Balacco [a,*], M.R. Alfio [a], M. Arfaoui [b], D. Bassukas [c], C. Güler [d], F. Hamzaoui-Azaza [b], C. Külls [c], A. Panagopoulos [e], A. Parisi [a], E. Sachsamanoglou [f], E. Tziritis [f]

[a] Civil Environmental Land Building Engineering and Chemistry Dept. (DICATECh) Polytechnic University of Bari Bari Italy
[b] Laboratory of Sedimentary Basins and Petroleum Geology (SBPG) LR18 ES07 University of Tunis El Manar Faculty of Sciences of Tunis Tunis Tunisia
[c] Technische Hochschule Lübeck Laboratory of Hydrology and International Water Management Lübeck Germany
[d] Mersin University Faculty of Engineering Department of Geological Engineering Yenişehir Mersin Turkey
[e] Hellenic Agricultural Organisation (HAO) Soil & Water Resources Resources Institute Thessaloniki Thermi Campus Greece
[f] Hellenic Agricultural Organisation (HAO) - General Directorate of Research Soil and Water Resources Institute Gorgopotamou Str Sindos Greece

ARTICLE INFO

This manuscript was handled by Huaming Guo, Editor-in-Chief, with the assistance of Mingjie Chen, Associate Editor?.

Keywords:
Chloride
Groundwater salinization
Coastal aquifer
Cumulative probability
Nitrate
Background level

ABSTRACT

Seawater intrusion is the primary cause of groundwater salinisation in coastal aquifers. However, attributing salinisation solely to seawater intrusion may not always be accurate, given the likely presence of other sources. To understand if salinisation comes from seawater intrusion and its onset is crucial for groundwater management, but there are no definite threshold values for common indicators such as chlorides. Based on 1662 groundwater analyses from five Mediterranean coastal aquifers, the study aimed to distinguish the effects of mixing with present-day seawater from those caused by other sources. The trend analysis of cumulative probability plots of chloride (and total dissolved solids) is a key method for discriminating different groundwater salinisation sources and processes. Results establish that chloride, as a non-reactive tracer, is a more reliable indicator of seawater intrusion than total dissolved solids, a reactive indicator.

A chloride concentration threshold of 200 mg/L identifies the seawater intrusion onset. The threshold validation comes from groundwater salinisation facies, as provided by groundwater-type codification.

Fresh groundwater (Cl < 200 mg/L) anomalous total dissolved solids highlight the input of non-chloride salts and pollutants, providing caution regarding using total dissolved solids to recognise seawater intrusion. Beyond the threshold (Cl > 200 mg/L), data disclose emergent signals of salinisation sources and water–rock interaction processes overlapping seawater intrusion or the involvement of saline fluids different from present-day seawater. The threshold and a new categorisation of groundwater in coastal aquifers according to salinisation processes provide a benchmark for identifying and managing seawater intrusion in the Mediterranean area.

1. Introduction

The Mediterranean region includes many coastal aquifers (Calaforra, 2005; Calaforra et al., 2005; Tulipano et al., 2005), Where rising water demand and excessive groundwater extraction significantly affect both environmental and socio-economic conditions (Leduc et al., 2016). In most regions, irrigation constitutes the primary consumer of water. Certain areas are particularly dependent on groundwater resources for potable water and tourism, resulting in significant demand surges during the summer months. When coupled with the general uncertainty about climate change and sea-level rise projections (Colombani et al., 2016), and desertification (Verstraete et al., 2009), as well as the effects of entangling human activities such as land use changes, hydraulic works, and artificial inflows/outflows, the current groundwater status in coastal areas raises concerns regarding both the quantitative (water shortage) and qualitative (salinization and pollution) aspects.

Researchers and managers usually expect by default that the cause of groundwater salinization in coastal aquifers is present-day seawater intrusion.

However, various processes and salinization sources beyond present-

* Corresponding author.
E-mail address: gabriella.balacco@poliba.it (G. Balacco).

https://doi.org/10.1016/j.jhydrol.2025.132775
Received 4 October 2024; Received in revised form 14 December 2024; Accepted 18 January 2025
Available online 3 February 2025

day seawater can lead to an increase in groundwater salinity. In groundwater, we may observe significant levels of chloride concentrations, Electrical Conductivity (EC), or Total Dissolved Solids (TDS) without any or minimal influence from present-day seawater intrusion due to factors such as evaporite (including non-chloride salts) dissolution and leaching, mixing with saline and thermal fluids, irrigation return flow (creating basin closure and salt enrichment), reverse osmosis, input of salt spray, leakage of brines and numerous other sources (Mastrocicco and Colombani, 2021). Furthermore, in addition to the traditional view, contemporary anthropogenic sources emerge as the primary cause of the Freshwater Salinization Syndrome (FSS), which is a widespread and systemic water quality issue (Kaushal et al., 2021).

Within this framework, groundwater salinization (GWS) is a general term that denotes the effects of processes or salinization sources (natural or nonnatural) leading to a change in the concentration of dissolved solids in comparison to the natural levels observed in unaffected areas. To specifically address the impact of mixing with present-day seawater (or with saline fluids derived from seawater), we will utilize the term SSW (Salinization by Sea Water). We anticipate a mixing process with such fluids to impart features to chloride concentrations distinguishable from those caused by other possible processes and sources producing salinization.

Regarding SSW, the critical question is: Which chemical component of groundwaters can indicate the involvement of present-day seawater? Chloride serves as the primary non-reactive tracer of SSW. There is no direct substitute for using its concentration to monitor its progress unless we turn to more sophisticated geochemistry, which depends on comprehensive analyses, minor elements, and isotopes capable of distinguishing between various sources and processes of salinization (Vengosh, 2003). When it comes to the selection of chloride, a fundamental question arises: Can we establish a reliable chloride threshold to accurately indicate the onset of SSW and develop a classification system for a preliminary screening of groundwater salinity conditions based solely on minimal chemical analyses (major elements, which are the most analysed elements and available in historical datasets)? This straightforward approach, if implemented, could help avoid inaccurate interpretations about the presence of seawater intrusion (false positives) that often lead to wrong management interventions. Such an approach could be a game changer for countries with limited resources for groundwater monitoring, prompting a reconsideration of the default use of chloride, EC, and TDS in identifying seawater as the groundwater salinization source.

Some may argue that existing classifications already established the SSW salinisation threshold for groundwater in coastal aquifers. The Stuyfzand (1986) classification establishes the threshold for fresh water at 150 mg/L, corresponding to the drinking water standard in the European Community in the 1980 s. On the other hand, Giménez-Forcada (2010) does not specify a chloride threshold but selects the chloride concentration of the freshest water in each study site to define the freshwater component in the Hydrochemical Facies Diagram. The literature concerning SSW does not reveal other attempts at defining a general chloride threshold, commonly set as equal to the Water Quality Standards (WQS) of chlorides in force in different countries for drinking purposes or to the WQS of international organizations (EPA, 2024; WHO, 2022; EU, 2020). Sometimes, the threshold is expressed only in terms of TDS or EC. Even the classic Revelle index (Revelle, 1941), which indirectly defines the threshold of SSW by considering the ratio between chlorides and dissolved carbonated species and constitutes the base for evaluating the impact of seawater intrusion in vulnerability mapping methods (e.g., GALDIT; Chachadi and Lobo Ferreira, 2001) does not specify any chloride threshold. In the same vein, countless water quality indices, and the Seawater Mixing Index (Seh-Chang et al., 2005) use combination of parameters and ion ratios, but they do not identify any specific chloride threshold.

Some might reason that we could establish the chloride threshold with the procedures used to recognize the natural background levels (NBLs, e.g. “the concentration of a substance in an environmental medium (air, water, or soil) that occurs naturally or is not the result of human activities”, EEA, 2024). Pulido-Velazquez et al. (2022) find different NBLs for chlorides in some European coastal aquifers. Their task is more complex than usual because, according to the NBL’s procedure, only pristine, unpolluted waters should be considered, and seawater intrusion represents an additional impact that needs to be addressed. As anticipated, chloride NBLs differ among the coastal aquifers studied due to variations in pristine waters caused by local hydrological and hydrogeological constraints.

The literature review highlights that a chloride concentration threshold for SSW of general significance, not based on water standards, has yet to be defined. To fill this gap is precisely this study’s primary objective. Our research aims to understand how the mixing of present-day seawater affects chloride concentrations in groundwater. We analyse these concentrations to distinguish the impacts of seawater and saltwater mixing from other sources of salinization, including human activities.

We use cumulative probability (CP) and box plots to recognize the chloride threshold for SSW using a chemical analysis dataset concerning five Mediterranean coastal aquifers located in Greece, Italy, Turkey, and Tunisia.

Generally, the construction of a CP plot requires a minimum of about 100 data values, although techniques are available for dealing with fewer data. Considering the potential challenges linked to small datasets, we did a thorough effort to reduce uncertainty and bolster statistical power by collecting all pertinent historical chemical analyses for each considered aquifer. Even considering only basic water quality parameters, comprehensive datasets can unveil subtle yet important patterns and clues that might not be apparent in smaller, even more complete datasets. Historical data, often incomplete and with varying accuracy and precision, and samples frequently needing more metadata for their validation pose a challenge in hydrogeological research. Thus, meticulous scrutiny of such data is essential to ensure accuracy and prevent misleading conclusions.

We also define a straightforward hydrogeochemical labelling of groundwater samples based on major elements to support the threshold choice. Combining the information concerning the chloride salinization threshold, the water labelling, and the natural background levels of nitrates and sulphates we define a new categorization of groundwater in coastal aquifers.

Finally, our study aims to achieve the following objectives: 1. Distinguish the effects of mixing with present-day seawater from those caused by other sources, including human activities, using CP plots of common indicators like chlorides and TDS; 2. Validate the selection of a threshold by combining CP results and water-type labelling; 3. Group and categorize groundwater samples according to groundwater salinization processes, supporting the choices with the analysis of nitrate and sulphate statistical distribution.

2. Materials and methods

2.1. Test sites

The five aquifers selected as test sites (Appendix A: Fig. A.1) are representative of a variety of Mediterranean groundwater salinization sources and processes while showing diverse hydrogeological framework complexity (Table 1). They are the Rhodope aquifer system (RHO, Greece), the Bouficha aquifer (BFC, Tunisia), the Salento aquifer (SAL, Italy), the Samos aquifer (SAM, Greece) and the Tarsus aquifer (TAR, Turkey). The five aquifers differ concerning size, geographical, geological, lithological, and structural features, which condition permeability, type of water–rock interaction processes and salinization sources (Balacco et al., 2022; Cotecchia, 1977; Cotecchia, 2017; Demirel, 2004; Demirel and Güler, 2006; Fidelibus and Pulido-Bosch, 2019; Güler et al., 2012; Galazoulas et al., 2011; Hamzaoui-Azaza et al., 2020; John and

Table 1
Major hydrogeological features of the test sites.

Study Areas	Bouficha (BFC)	Rhodope (RHO)	Salento (SAL)	Samos (SAM)	Tarsus (TAR)
Country	Tunisia	Greece	Italy	Greece	Turkey
Aquifer(s)	Superficial aquifer	Two hydraulically interconnected aquifers (upper/lower)	Karst aquifer of regional extension	Shallow aquifer	Aquifer system with confined (upper) and semi-confined (lower) aquifers
Geology	Sandy-clayey and conglomerate deposits (Quaternary)	Upper (semi-confined) aquifer: Alluvium deposits of sand, gravel, and pebbles. Lower (confined) aquifer: Coarse-grained alluvial sediments (Miocene-Pliocene)	Cretaceous limestone and dolomitic limestone	Quaternary alluvial gravel	Upper aquifer: Unconsolidated fluvial-deltaic sediments with intercalation of thick clay-silt layers or lenses (upper).Lower aquifer: Quaternary deposits (lower)
Thickness (m)	up to 500	30–130	Around 3,000	20—30	30—500
Surface areaextension (km^2)	50	165.1	2799	20	240.1

Krivy, 1965; Kallioras et al., 2006; Mountrakis et al., 2003; Petalas and Diamantis, 1999; Stamatakis et al., 2009; Tziritis et al., 2023). The thicknesses and the surface dimensions in Table 1 refer to each entire system. The systems decrease in size from SAL to SAM. SAL is a karst aquifer where groundwater primarily circulates in phreatic conditions. The RHO system consists of an upper semi-confined aquifer and a deeper confined aquifer. The TAR system includes one confined (upper) aquifer and one semi-confined (lower) aquifer. The BFC aquifer is a shallow aquifer with limited surface extent, while SAM is a shallow aquifer with modest thickness and surface dimension. Freshwater circulation, which occurs along local, intermediate, and regional flow systems (Toth, 1963) consistently with the system structure, hydraulic heads, and consequent freshwater-saltwater equilibria, does not affect all the systems' thickness. Groundwater shows differences in residence time and mineralization because of the control exerted by flow systems on the time response to seasonal and human pressure variations. Despite the differences, the test sites share similarities regarding palae-geography, climate, water use, natural and anthropic pressures. Details about the test sites are in Appendix A.

The economic conditions and management rules of the different study sites have significantly influenced their approaches to controlling environmental variables over time. All sites face challenges related to a variable equipment of monitoring wells, spatial coherence of groundwater monitoring networks, regularity of controls, parameters analysed, methodologies for sampling and analysis as well as quality of data. As a result, while they all require improved data—albeit to varying degrees—the existing data is frequently insufficient for a comprehensive analysis of issues as groundwater salinization.

2.2. Collation and quality control of data

To address the challenges of comparing data across various sites—due to differences in volume, spatial and temporal distribution of groundwater chemical data, hydrogeological frameworks, groundwater composition, monitoring practices, and the range of sampling and analytical methods—we focused on enhancing the numerical dataset by gathering archived data from these locations to create a comprehensive database.

The historical database (DB) from the test sites includes chemical analyses from monitoring for environmental reference/baseline, compliance with regulatory standards, or scientific research.

In most instances, there was no metadata concerning historical chemical analyses, making it challenging to identify the stratigraphy, well depths and equipment, and the sampling methods used. The available metadata indicates that the samples were primarily collected by pumping from wells for domestic or irrigation use, with some instances involving the interconnection of multiple aquifer levels. Sampling depths cannot be defined because the elevation of the pumps is generally unknown. This way, samples generally do not represent groundwater from a single aquifer level. This situation is common worldwide, and using bailers for sampling is infrequent and not deemed essential, even for scientific research. In BFC, RHO, SAM, and TAR, sample collection mainly occurs through pumps because most wells are private wells. Only the SAL aquifer-related samples, where the monitoring well net belongs to the regional government, refer to specific depths owing to using bailers because wells are free from pumps.

However, the lack of information does not prevent the use of such historical data for statistical purposes. The information we search for is embedded even in "poor" data because we are interested in making the signals of salinisation processes emerge.

The validation of the collected chemical analyses first concerned their completeness (i.e., the inclusion of the major ions Ca^{2+}, Mg^{2+}, Na^{+}, K^{+}, Cl^{-}, SO_4^{2-}, HCO_3^{-}), a good level of precision and accuracy of measures and the fulfilment of the criterion of $-10\ \% < CBE < +10\ \%$ (Charge Balance Error). The validated final DB consisted of 1,662 chemical analyses, 1,292 of which refer to historical data and 370 to samples collected in 2020–2021 during ten sampling surveys conducted across the five study areas.

Samples represent fresh, salinised, and saline groundwater. One thousand five hundred sixty-eight (1,568) samples pertain to groundwater sampled from 699 wells: such sub-set includes salt waters sampled beneath transition zones and saline fluids from deep wells. Out of the remaining 94 samples, 45 are from inland and coastal springs, 41 refer to rivers, natural and artificial lakes, irrigation and draining canals, reservoirs and dams and eight represent modern seawater sampled offshore at the test sites- The spring waters and seawater represent valuable references as fresh or saline end-members of the mixing process. The surface waters, commonly utilized for irrigation, span from fresh to brackish and either recharge groundwater or receive recharge from it. In light of the significant relationships with groundwater, their waters also constitute potential end-members of the salinization processes and have been incorporated into the database for comprehensive statistical analysis. Table 2 details the sample count per type of sampling point for each test site. Samples refer, in some sites, to even more than two decades (Table 2), which include major periods of persistent droughts. This occurrence is significant from the hydrogeological point of view because droughts stress the aquifers, as highlighted by Cook et al. (2016) for the Mediterranean area, and may induce transient salinization processes linked to sources that otherwise do not emerge.

All chemical analyses comprise the major ions. Concentrations of sulfate and potassium, when (rarely) under the limit of detection (LOD), have been substituted by 0.55 times the LOD (see Sanford et al., 1993) for further statistical processing. Most analyses (96 %) do not report laboratory-measures of TDS. To fill the gap, it was calculated with PHREEQC Interactive ver. 3.1.4 (Parkhurst and Appelo, 2013) based on concentration of major ions. 90 % of the analyses include nitrates, and 11 % do not include Electrical Conductivity (EC).

The DB only considers chemical analyses that meet the criterion of $-10\ \% < CBE < +10\ \%$ (Charge Balance Error). The CBE values concerning the 1,662 analyses (Appendix A: Fig. A.2a) are equally distributed around zero for waters with TDS > 1,000 mg/L, while positive CBEs prevail for waters with TDS < 1,000 mg/L.

Table 2
Samples reference period and sample count per type of sampling point for each test site.

TEST SITES	BFC	RHO	SAL	SAM	TAR	Total samplesper type
Period	2021	1993–2021	1985–2021	2008; 2020–2021	2008; 2020–2021	
Groundwater samplesfrom wells	49	463	632	140	284	1568
Spring water samples			28	17		45
Surface water samples	3			13	25	41
Seawater samples	2		3		3	8
Total samples	52	463	660	170	309	1662

The chloride concentration of the whole DB ranges from 6 to 24,106 mg/L, and TDS from 50 to 46,116 mg/L, thus spanning over five orders of magnitude. Table 3 shows the maximum and minimum values of major ions, nitrates and TDS for the only groundwater samples of each test sites.

The DB was generated in the context of MEDSAL project (www.medsal.eu) and is available at the MEDSAL Web Observatory (https://openmedsal.eu/), which constitutes an open-access web-GIS tool for monitoring GWS in Mediterranean aquifers.

3. Methodology

The rationale behind collating archive data from the test sites in a unique, comprehensive DB was that such a DB would encompass a broad spectrum of chemical parameter concentrations reflecting a range of groundwater salinisation processes and sources.

Conducting a probabilistic study, which does not rely on assumptions about the underlying data distribution, may yield valuable insights relevant to our research objectives by identifying common controlling factors associated with salinisation sources. Certainly, salinisation due to seawater/saltwater mixing is, among such controlling factors, relevant for all five aquifers. The frequency distribution of selected parameter values and variations in the cumulative frequency curves—free from arbitrary or subjective estimates—could be an effective exploratory tool for our analysis.

The data processing, developed in successive steps, entails the analysis of the Cumulative Probability (CP) plots (Sinclair, 1974; 1976) of chlorides and TDS, the water-type labelling, the analysis of the CP plots of nitrate and sulphates, and setting the rules for the categorization of groundwater in coastal aquifers.

The first step, a purely statistical approach, establishes the value of the chloride salinisation threshold for SSW and finds the limits of statistical populations corresponding to changes in the GWS processes. The second step deals with labelling each groundwater sample: it is essential for validating the analysis results concerning the previous CP plots. The third step helps establish the Natural Background Levels of nitrates and sulphates, which, coupled with earlier information, leads to groundwater's final categorisation.

3.1. Establishing a salinization threshold

CP plots have been initially used in exploration geochemistry (Tennant and White, 1959; Lepeltier, 1969). CP and box plots are efficient methods of deriving pollutant and trace element NBLs because they provide unbiased statistical data (Edmunds et al., 2003; Reimann et al., 2005; Panno et al., 2006; Sajil Kumar, 2017). On a CP plot, data are plotted on the x-axis against the cumulative probability (i.e., the scale on the y-axis expressed in probabilities). With a linear scale for the x-axis, one may tell whether the data are close to being normally distributed as the data will track a straight line. With a logarithmic scale for the x-axis, log-normal populations (but also normally distributed populations with a small coefficient of variation) will plot as straight lines. We will use an x-log scale because most parameter values, including those of chloride and TDS, cover many orders of magnitude.

Large regional geochemical and environmental datasets often do not follow a normal or log-normal distribution. Instead, multiple processes or sources likely influence these extensive datasets, resulting in polymodal distributions (Reimann and Filzmoser, 2000). Such distributions generally combine two or more (normal and log-normal) populations (Sinclair, 1974; Limpert et al., 2001). The poly-modal distributions observed in groundwater chemical data can help distinguish between different types of groundwater based on the assumption that these various populations originate from distinct geochemical processes (Rahman et al., 2021).

The CP plot of a polymodal distribution with a log x-axis shows a series of linear trends delimited by changes in slope. The inflection points (Sinclair, 1974, 1976) allow identifying the single populations (partitioning method). Sometimes there is a gradual transition between the linear trends, corresponding to a mixed population because of the overlapping of two normal or log-normal populations. However, the Kolmogorov–Smirnov test of normality and calculation of skewness help evaluating the most likely approximation to a normal or log-normal population.

The basic assumption is that the changes in slope in the polymodal CP plots of chlorides (and TDS) will aid in identifying the different salinization processes responsible for the increase in chloride concentration (and TDS), including the groundwater–seawater (or saltwater) mixing.

Table 3
Minimum and maximum concentrations of major ions and TDS for the groundwater samples of each test site. Nitrate values refer to the 90% of samples.

		BFC		RHO		SAL		SAM		TAR	
Number of GW samples		49		463		660		157		284	
		min	max	min	max	min	max	min	max	min	max
Ca^{2+}	mg/L	78	678	4.0	4,328.6	3.7	945	6.5	737	8.4	671.7
Mg^{2+}	mg/L	50.4	431.8	1.5	962.3	1.5	1,680	0.5	831.7	4.6	766.6
Na^{+}	mg/L	143.8	2,363.3	7.9	4,655	5.0	14,000	5.1	7472	10	3,283
K^{+}	mg/L	1.2	127.9	0.7	184.6	0.1	6,300	0.4	382	0.7	216.9
Cl^{-}	mg/L	267.7	3,807.7	7.3	12,928.6	13.0	24,106	10.2	12,372	7.6	6,070
$SO_4^{=}$	mg/L	39.2	2,952	2.5	923	0.8	6,600	5.3	1,939.5	1.0	1,004
HCO_3^{-}	mg/L	230.6	788.2	27	927.2	9.0	722	21.4	615.9	140.7	886
NO_3^{-}	mg/L	0.5	202.7	0.1	229.2	0.1	130	0.1	49.6	0.1	201.1
TDS	mg/L	906.7	9,720	194.5	20,563.2	167.2	46,116.1	56.6	22,689	304	3,283

3.2. Methodology for water-type labelling and categorization of groundwater in coastal aquifers

The water labelling considers typical chemical water types that develop during seawater intrusion and recharge phases in coastal aquifers (Appelo et al., 1990; Appelo and Postma, 2005). These phases induce the exchange of Na/Ca (inverse) and Ca/Na (direct) ions, driven by even minute quantities of exchangers like clays, which possess a significant specific surface area for ion exchange.

The Na/Ca inverse exchange occurs when seawater displaces freshwater: the exchanger-water system reacts, inducing the release of Ca^{2+} (occupying a significant proportion of exchange sites) and the simultaneous adsorption of Na^{+} (Howard and Lloyd, 1983). The Na/Ca exchange leads to the typical CaCl hydrochemical water type. The Ca/Na direct exchange occurs when recharge waters flush the salinised aquifer sediments (where clays retain a high proportion of adsorbed Na^{+}) (Appelo and Geirnaert, 1983; Lloyd and Heathcote, 1985; Tellam et al., 1986). The Ca/Na exchange leads to $NaHCO_3$ water type as the flushing final term (see Appelo and Willemsen, 1987; Beekman, 1991; and Giménez and Morell, 1997 for details of water types and their sequences). Under natural conditions, seawater intrusion and recharge occur cyclically in coastal aquifers without reaching, in most cases, their complete evolution. Furthermore, the flow reversal shows hysteresis and does not restore the water's chemical quality to its previous conditions, as the ion-exchange processes are not linear. The Stuyfzand (1986) classification and the Hydrochemical Facies Evolution Diagram (HFE-Diagram) (Giménez-Forcada, 2010; Giménez-Forcada, 2014; Giménez-Forcada and Sánchez San Román, 2015) have the merit of describing the dynamics of salinization based on such concepts.

We draw inspiration from such classifications to establish straightforward rules for water-labelling.

To be specific about the study, which is focused on salinization processes, we use the term Salinization Facies (SF) instead of the more well-known and widespread Hydrochemical Facies to identify water types.

The labelling involves the construction of a SF acronym. The first step of water labelling involves defining the Main Type and the first index (prefix) of the SF acronym based on the chloride ranges of different populations and the SSW chloride threshold derived from the CP plot analysis. In the second step, we identify the most abundant cation, which defines the second and third indexes qualifying the Sub Type. This process needs the beforehand calculation of the concentrations of major ions (including nitrates) in meq/L. Then, we determine the percentage share of each cation relative to the total sum of cations. The percentage predominance of either the sum of alkaline or alkaline-earth ions facilitates the definition of the second index (namely, Na, Ca, Mg, CaMg, and MgCa). The third step involves recognizing the most abundant anion by calculating the percentage share of each anion compared to the total sum of anions. The step defines the third index (i.e., Cl, HCO3, SO4, MixCl, MixB, MixS, and MixN). Fig. 1 shows the steps for the SF acronym construction and two water labelling examples. The procedure is applied to each of the 1662 samples of the DB from all the test sites, regardless of the type of sampling point. It cannot be applied a priori and is strictly consequent to the definition of the limits of the

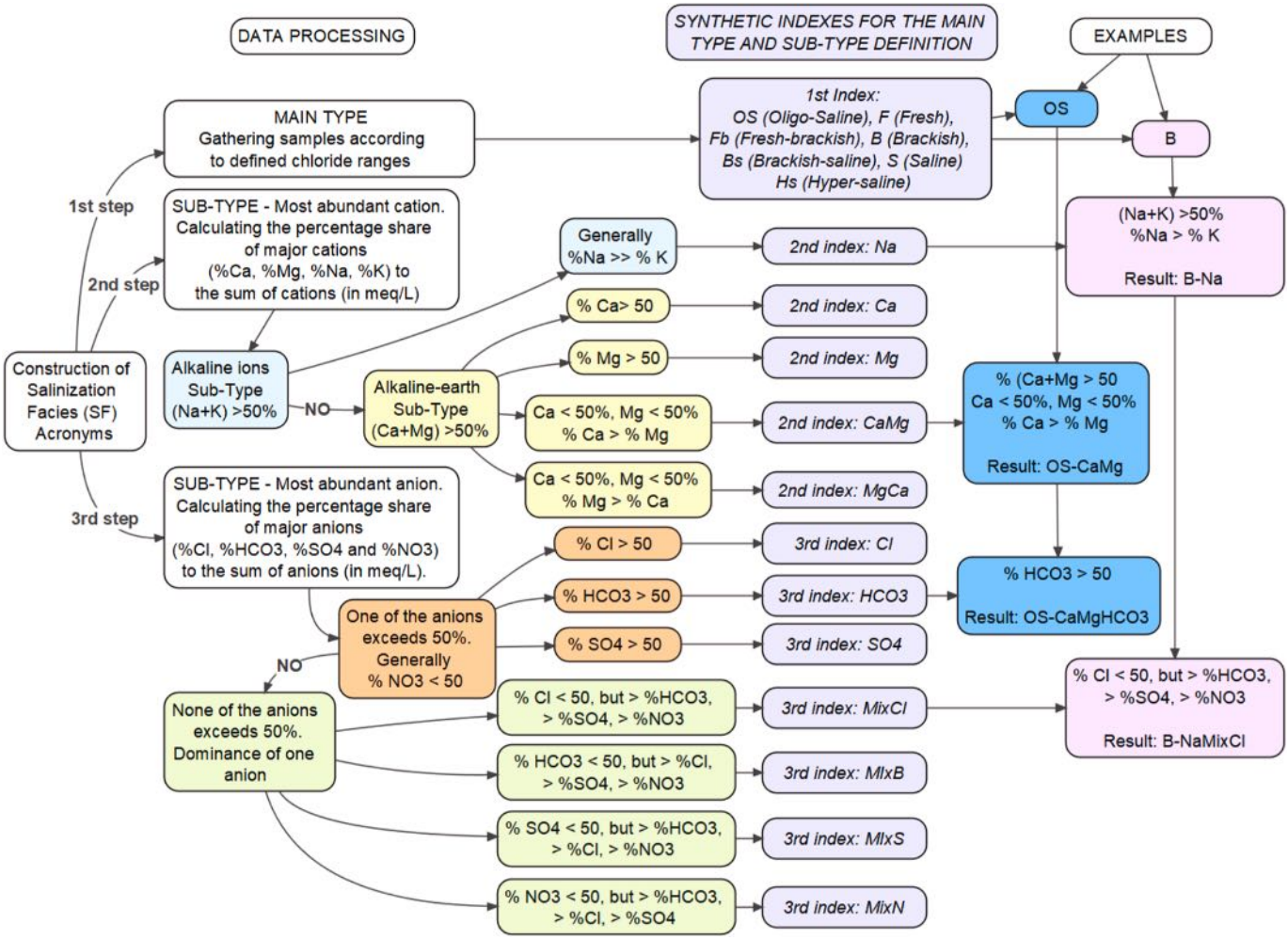

Fig. 1. Steps for constructing the Salinization Facies acronym.

statistical populations and the definition of the SSW operated through the thorough analysis of the CP plots of the chloride and TDS concentrations. We can review the variations of the SFs in light of the usual water–rock interaction processes and those illustrated above, which activate during freshwater-seawater mixing. Once the SSW threshold and the limits of the statistical populations from the CP plots are defined, the SFs falling before and after the threshold and in the specific groupings can help validate the former.

We cannot define the rules for categorising groundwater in coastal aquifers in advance, as these depend on validation with the salinisation facies resulting from the statistical analysis. The categorisation focuses on freshwater and groundwater with chloride concentrations that are close to, but just above, the threshold. The goal is to highlight the differences between saltwater intrusion (SSW) and other groundwater salinisation (GWS) processes. The categorisation procedure also utilises CP plots of nitrate and sulfate, with nitrate being considered an indicator of GWS influenced by human activities.

4. Results

4.1. Cumulative probability plots, salinization thresholds and groundwater categorization in SFs

Fig. 2 shows the CP plot for chlorides while Fig. 3 shows the CP plot of TDS (in mg/L). The plots are based on 1,654 out of the 1,662 samples of the DB because of the exclusion of the eight seawater samples. The Cl and TDS distributions are not normal, as expected, showing a skewness of 3.70 and 3.81, and a p-value of the Kolmogorov–Smirnov test for normality less than 0.05.

Examining the poly-modal trends of the Cl and TDS CP plots we recognize nine (corresponding to groups from 1 to 9 in Fig. 2) and four linear trends (A, B, C, and D in Fig. 3), respectively. Such groups, corresponding to distinct statistical populations, are recognized by changes in the CP plot slope. The inflexion point's precise pick-up (by visually inspecting), which should correspond to the intersection of two populations, may take work. Thus, the partitioning proceeds as a trial and error-process. The type and limits of the recognised single populations are validated by the linearity of their CP plots and by Kolmogorov–Smirnov test for normality.

The box plots for the chloride and TDS groups are shown in Fig. 4. Table A.1 and Table A.2 in Appendix A show the related statistics, respectively. The single CP plots (Fig. 2) of the nine chloride groups correspond to normally distributed populations. The closeness of their means and medians, their skewness in the range from −0.5 to + 0.5, and the p-value of the Kolmogorov–Smirnov test for normality higher 0.05 demonstrate this normality (Appendix A: Table A.1).

The data are too few to be statistically significant below the lower limit of Group 1 (Cl < 25 mg/L). Between each pair of groups (except the contiguous groups 4 and 5), the CP plot shows gradual transitions because of overlapping populations (in the following named OP 1–2, OP 2–3, etc.). The most significant slope change in the CP plot of chlorides (Fig. 2) occurs at the 51st percentile (Cl = 200 mg/L). We attribute such a slope change to the onset of SSW. The trend is irregular above the upper limit of Group 9 (Cl > 2000 mg/L), suggesting a concurrent contribution of various salt sources/processes. The groups A, B, and D in Fig. 4 correspond to normally distributed populations, while the group C is log-normal (Appendix A: Table A.3). Fig. 3 shows gradual transitions between adjacent TDS groups (OP A-B, etc). Two crossing lines highlight a significant slope change (Fig. 3) around the 39th percentile (TDS = 700 mg/L). Beyond the upper limit of Group D, there are no significant trends, likely because we come across the realm of complex overlapping salinization processes.

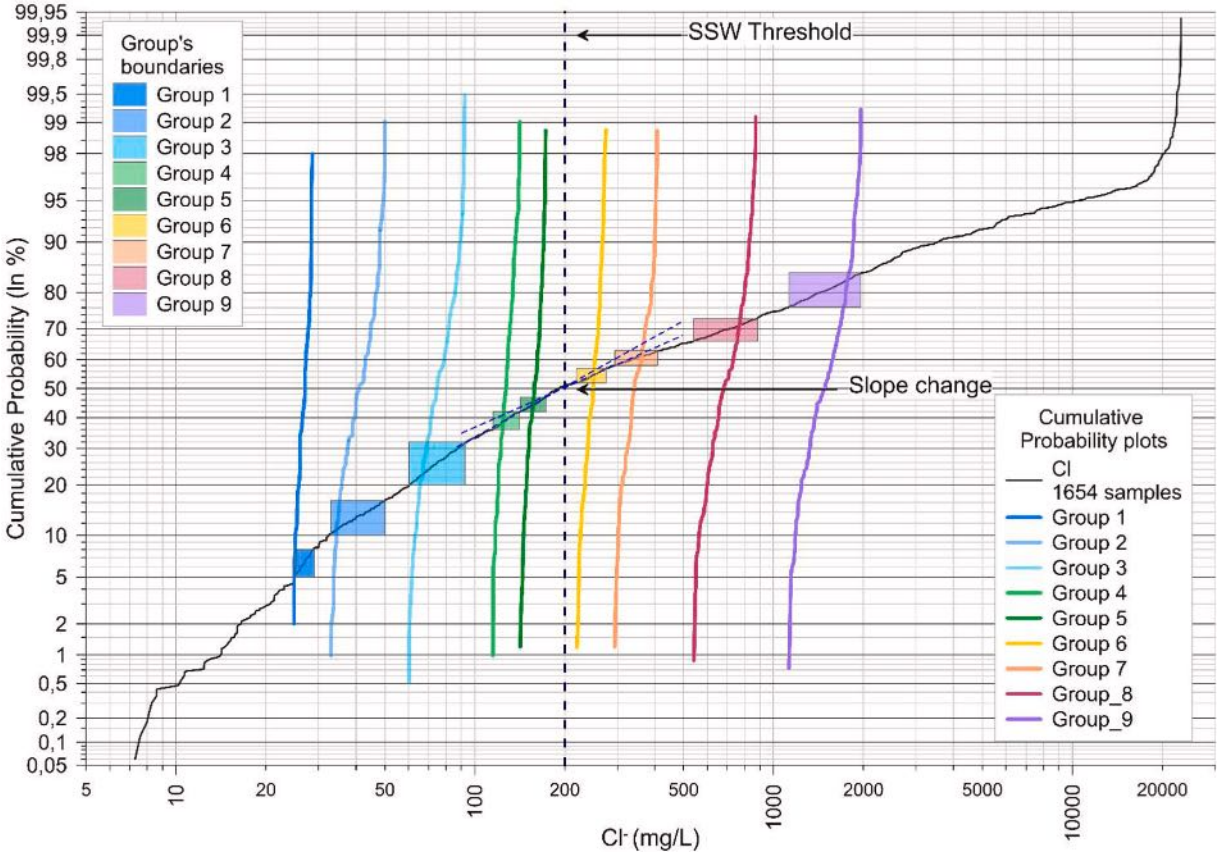

Fig. 2. Cumulative probability plots for Cl (mg/L), Groups and single CPs of the related populations. The crossing dotted lines mark the position of the primary slope change at the 51st percentile.

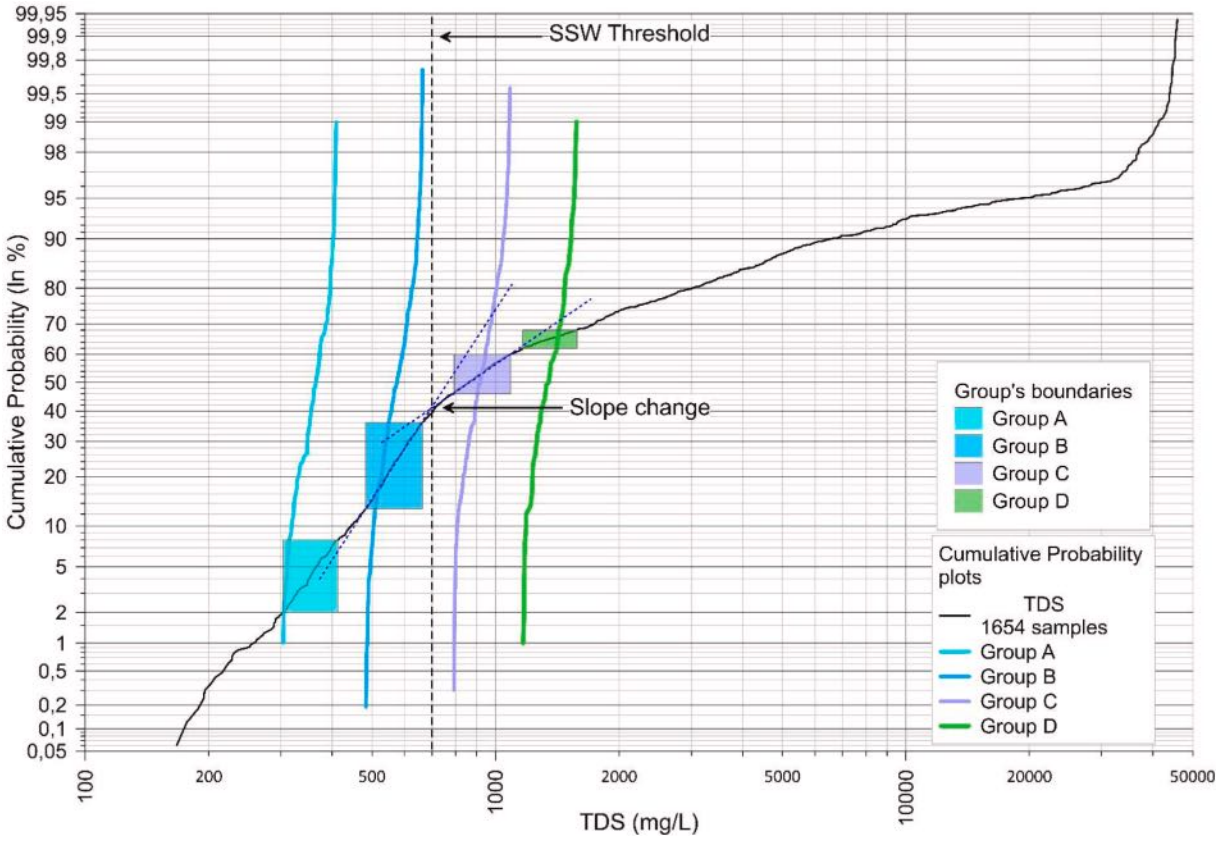

Fig. 3. Cumulative Probability plot of TDS (mg/L) and related groups. The crossing dotted lines mark the position of the primary slope change at the 39th percentile.

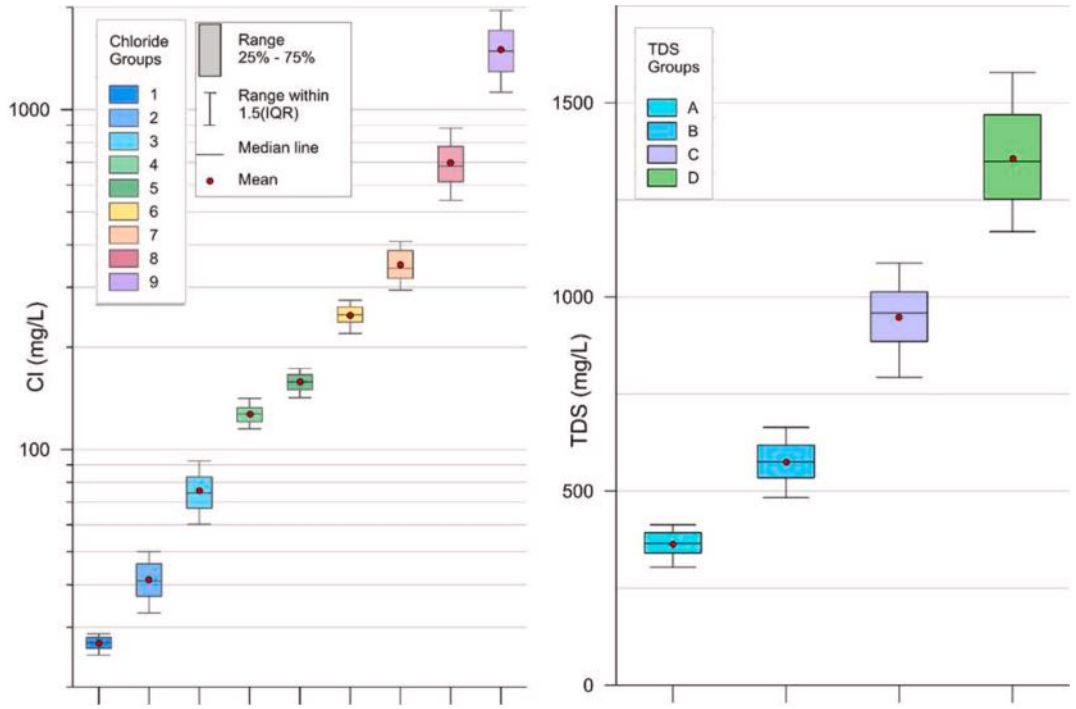

Fig. 4. (left) Box plots of chloride groups based on the Cumulative Probability plot of chloride (Fig. 2) and (right) of TDS Groups based on the Cumulative Probability plot of TDS (Fig. 3).

Both the CP plots of Cl and TDS reveal a significant change in slope caused by a substantial shift in the primary process leading to groundwater salinization, which divides each plot into two distinct areas. We observe that the information about salinization processes differs between the two considered parameters. The Cl CP deals with concentrations of a single anion, while the TDS CP plot considers the sum of all

major cations and anions concentrations. Consequently, when they are affected by the same input sources or mixing processes their increase follows different paths. Chloride concentration mainly increases because of the dissolution of chloride salts and mixing with saline fluids.

The TDS increases because of the summing-up of the effects of the previous factors and a multiplicity of overlapping salinization sources (including non-chloride salts) and WRI processes, mainly triggered by the increase in ionic strength. This condition classifies TDS as a 'reactive' (non-conservative) tracer of the GWS, while chloride is a non-reactive tracer (conservative).

These different features manifest when examining the linear correlation between chloride concentrations and TDS values. Even if the coefficient of determination is 0.99, the correlation coefficient is 0.997, and the *p*-value is less than 0.0001, the standard error of the estimate is significant (619.9 mg/L). In correspondence to the Cl CP slope change (200 mg/L), the linear correlation gives a TDS of 758 mg/L, close to the value of the TDS CP slope change (700 mg/L). However, the standard error, of the same order of magnitude of the estimated value, suggests that using an SSW threshold based on the TDS may be distorting because even the freshest groundwater with a chloride concentration lower than 200 mg/L may show a TDS higher than the TDS threshold. We may only use such a threshold as supporting information.

Our research findings support the reliability of using chloride as a non-reactive (conservative) tracer for mixing with seawater or saline fluids of marine origin. The most significant slope change at 200 mg/L points to a substantial change of source or process, causing the increase in chloride concentrations, which we interpret as the SSW threshold and the upper limit of freshwater.

Other salinisation processes affect freshwater at the left of the SSW threshold. Beyond the threshold, different WRI processes and salinisation sources may overlap with mixing, but the mixing with seawater or other saline fluids quantitatively prevails in imprinting groundwater features.

The SSW chloride threshold and the chloride groups allow defining the Main Types (MTs) of the SFs. To avoid gaps between the MTs chloride limits for categorisation and to align our findings for practical applications, we set each MT limits by considering not only data from chloride groups but also from overlapping populations. While the chloride CP plot shows distinct limits for groups associated with different processes that increase chloride levels, the main types do not adhere strictly to these boundaries. Instead, they incorporate data from one or more chloride groups, along with their overlaps. The limit between F and Fb waters corresponds to the chloride threshold, which, in turn, corresponds to the inflexion point between the chloride groups 5 and 6, centred in the overlapping population 5–6. The OS, F, and Fb MTs include either one or more of the chloride groups and part of the data of the overlapping populations contiguous to groups. Table 4 shows the limits of each MT and the included chloride Groups and Overlapping Populations.

After completing the SFs definition for each of the 1662 samples by defining also the Sub-Types, we analysed the SFs included in each MT e distinguished the SFs according to occurrence percentage into Dominant (higher than 10 %) and Subordinate (less than 10 %). The types and occurrence frequency of SFs included in each Main Type (Table 4) support the choice about the chloride SSW threshold. The −CaHCO3 SF dominates in the OS (Oligo-Saline) samples, while bicarbonate and −MixB SFs dominate in the Fresh (F) chloride range of 31–200 mg/L. Some of the subordinate SFs F-CaCl (and F-CaMgCl, F-MgCaCl, F-NaCl) observed within the F Main Type suggest an active salinization (phase of intrusion), which contrasts with the expected features of a F Main Type. However, these SFs represent only 6 % of samples, and we explain their appearance because of the inclusion of part of the overlapping population 5–6 samples. The chloride SFs become dominant within the Fresh-brackish (Fb) MT, after the chloride threshold. Beyond the limit of 1,000 mg/L of chloride, and for all B, Bs, S, and HS Main Types, samples show only chloride facies.

Table 4
Main Types of groundwater samples, their chloride range and Salinization Facies.

Main Types and included Groups	Cl (mg/L)	Dominant SFs	Subordinate SFs
OS (Oligo-Saline) Includes Group 1 and part of OP 1–2	≤30	OS-CaHCO3	OS-MgCaHCO3,OS-CaMgHCO3, OS-NaHCO3
F (Fresh) Includes: Groups 2, 3, 4, and 5; OPs 2–3, 3–4, 4–5, and part of OP 5–6	30 < Cl ≤ 200	F-CaMgHCO3 F-MgCaHCO3 F-CaHCO3F-CaMgMixB F-MgCaMixB	F-CaMgMixCl, F-MgCaMixCl,F-NaMixB, F-NaMixCl, F-NaHCO3, F-CaMixB, F-MgMixB, F-CaMgCl, F-MgCaCl, F-CaCl, F-NaCl,F-CaMgSO4,F-MgCaSO4,F-MgHCO3
Fb (Fresh-brackish) Includes: Group 6, 7 and 8; OPs 6–7, 7–8, part of OP 5–6 and 8–9	200 < Cl ≤ 1,000	Fb-NaCl, Fb-CaMgCl,Fb-MgCaCl, Fb-CaCl, Fb-CaMgMixCl	Fb-NaMixCl, Fb-NaHCO3 Fb-NaCl
B (Brackish)Includes: Group 9	1,000 < Cl ≤ 3,000	B-NaCl, B-CaCl	B-CaMgCl, B-MgCl
Bs (Brackish-saline)	3,000 < Cl ≤ 10,000	Bs-NaCl	Bs-CaCl, Bs-CaMgCl
S (Saline)	10,000 < Cl ≤ 20,000	S-NaCl	S-CaCl, S-CaMgCl
HS (Hyper-Saline)	>20,000	HS-NaCl	

4.2. Water quality issues of Oligo-Saline and fresh groundwater

The Chebotarev diagram (Chebotarev, 1955; Fig. 5a) shows the SFs of all DB samples. The −Mix SFs are not detailed with the Cl, B, S, and N suffixes to avoid displaying excessive symbols in the diagram.

The SF's distribution in Fig. 5a and the cross plots % (Na + K)-TDS (Fig. 5b) and % (Na + K)-Cl (Fig. 5c) emphasize a complex interplay between TDS, Cl, and chemical composition. The spreading of Oligo-Saline and Fresh waters in Fig. 5a evidence the (vertical) evolution from bicarbonate-alkaline earth to sodium-bicarbonate FSs and the (lateral) change from the former towards Mix FSs. We expect these changes because of the ion exchange during recharge (freshening) and the solution of chloride salts. Note that most of the FSs do not follow the FW-SW mixing line. The comparison of the OS and F FSs' position in Fig. 5b and c shows that the TDS of most of the F Mix FSs is higher than the TDS SSW threshold. As TDS and chloride increase after their respective thresholds, there is a significant departure of SFs from those expected from the FW-SW (non-reactive) mixing line. Contrary to the spreading around the FW-SW mixing line, which may be explained by the WRI triggered by mixing, that of the other samples suggests mixing with other saline fluids different from present-day seawater.

The complex nature of salinization beyond the SSW thresholds merits further analysis. Such data dispersion justifies why the CP plot of chlorides (Fig. 2) does not allow the recognition of evident normal or log-normal populations for Cl > 2000 mg/L and the CP plot of TDS does not show linear trends after group D (Fig. 3).

Fig. 6 shows that the information from groups based on chloride CP plot does not match the information from TDS groups. The previous considerations about the linear correlation between chloride concentrations and TDS values and the inadequacy of TDS as SSW indicator, find in Fig. 6 a further demonstration. Only the TDS Group A stays totally on the left of the chloride threshold. Group B's upper and right limits are close to the SSW TDS and chloride thresholds. Groups C and D include samples beyond both the chloride and TDS SSW thresholds. Chloride groups on the left of the chloride threshold (Groups 2, 3, 4, and

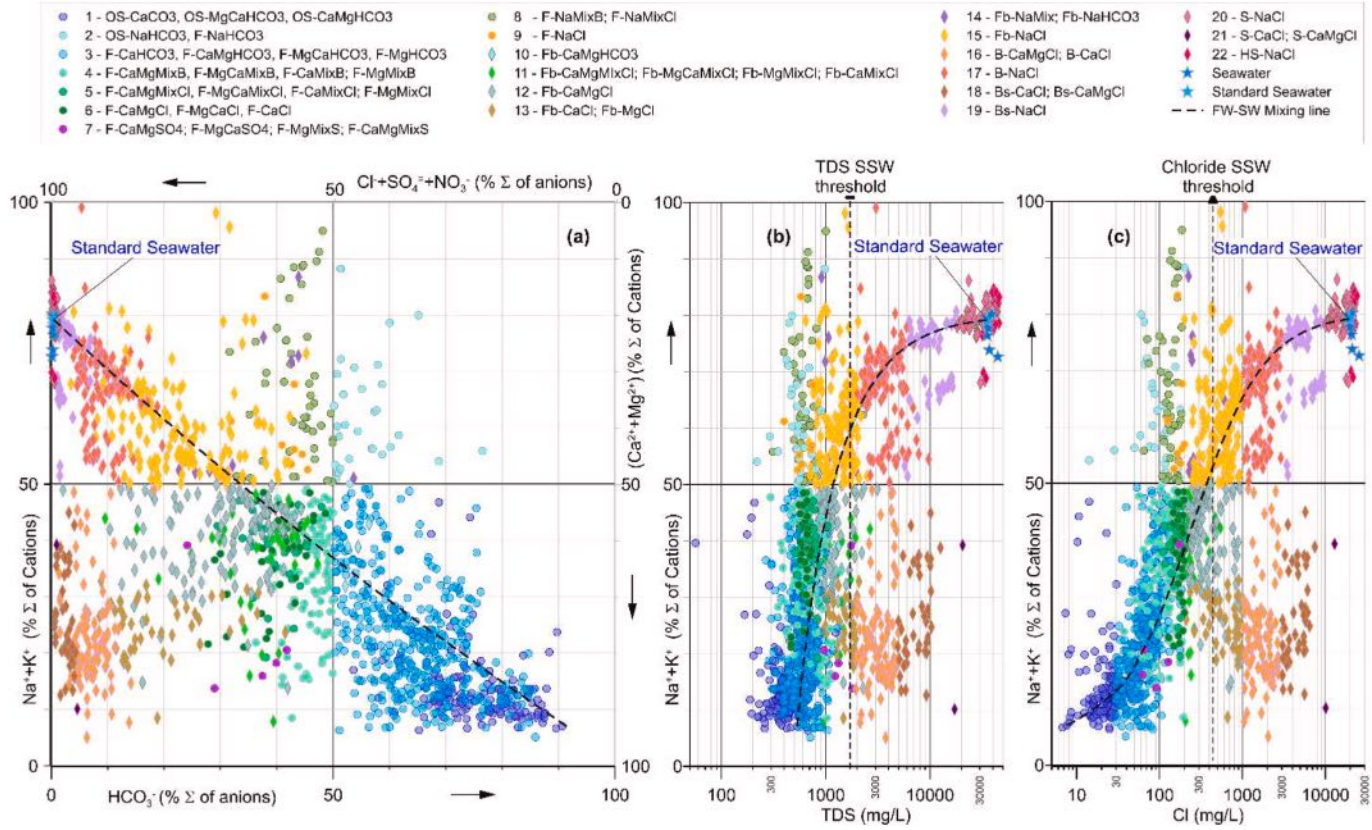

Fig. 5. (a) Chebotarev diagram of all DB samples; (b) Na + K (% sum of cations) vs. TDS (mg/L); (c) Na + K (% sum of cations) vs. chloride concentration (mg/L).

5) except Group 1 cross the TDS threshold, while Groups 6, 7, 8, and 9 are over it. In any case the SSW TDS threshold is ineffective in distinguishing fresh from SSW waters.

The high TDS values shown by freshwater beyond the TDS SSW threshold may depend on chloride increase because of the dissolution of natural or non-natural chloride salts (like KCl; Buvaneshwari et al., 2020) or irrigation return flow (solute recycling; Milnes and Renard, 2004). Moreover, domestic waste (e.g., septic tanks) in rural areas or manure can increase chloride concentrations (Garcia et al., 2012) highly correlated with nitrates. Nitrate and sulfate concentrations, reaching 155 and 740 mg/L, respectively, draw attention to the role of salt sources, such as $CaSO_4$ or fertilizers. The input of nitrates and sulfates and the concurrent cations such as calcium, potassium, or ammonium do not cause chloride concentration increase but impact on groundwater mineralization also by triggering additional WRI processes. This information is noteworthy as we are trying to shed light on the salinization processes often attributed to seawater intrusion without further thought. To this aim, we will combine nitrates (and sulfates) with chlorides and TDS to detail the groundwater categorization of Table 4.

The 90 % (760 samples) of the chemical analyses of the DB concerning only OS and F waters (844 samples) include nitrates, which we select as primary indicators of anthropogenic pollution. Nitrates mostly originate from human activities, including the use of nitrogen fertilizers, leakage from septic tanks, and release of effluents from wastewater treatment plants. All these human activities are likely sources of nitrates in the examined test sites. Nitrogen fertilizers may include chemicals as calcium ammonium nitrate ($5Ca(NO_3)2NH_4NO_3$), magnesium nitrate hexahydrate ($Mg(NO_3)_2{\cdot}6H_2O$), and ammonium sulfate ($(NH_4)_2SO_4$), whose dissolution increases the concentrations of Ca^{+2}, Mg^{+2}, NO_3^- (and SO_4^{2-}) ions in groundwater. Denitrification may cause low nitrate levels. Thus, waters subject to nitrate pollution may not appear so obviously linked to anthropic factors because of reactions that reduce the pollutant concentrations.

Sulfates come from both human activities and natural sources (Zak et al., 2021). Their concentrations have risen globally since the mid-20th century also because of complex reactions caused by nitrate leaching (Smolders et al., 2010). Therefore, we view sulfates as an additional indicator of human pollution. Anthropogenic sulfate comes from acid mine drainage, fertilizer such as gypsum ($CaSO_4{\cdot}2H_2O$), magnesium sulfate heptahydrate ($MgSO_4{\cdot}7H_2O$), ammonium sulfate ($(NH_4)_2SO_4$), sulfur-coated urea and elemental sulphur, overland drainage, and agricultural and industrial wastewater runoff. Natural sources include oxidation of sulfide minerals (e.g., pyrite), rainfall and volcanic activity, decomposition and combustion of organic matter, and sea spray aerosols, but high levels usually come from sulfate minerals (e.g., gypsum) and seawater intrusion.

We identified background values of nitrates and sulphates using the respective CP plots to sort concentrations of both ions concerning pollution. While the literature is rich with examples of nitrate Natural Background Level (NBL) estimations, the focus on sulfates is a less-trodden path. Sulfate NBLs have been established for regions of Northern and Southern Europe (Müller et al., 2006), Greece (Gemitzi, 2012), and Italy (Masciale et al., 2021) with the BRIDGE method (Müller et al., 2006). Lions et al. (2021) proposed a method considering the aquifer lithology to establish site-specific NBLs. Most methods consider only monitoring sites in pristine areas free from anthropogenic influence. The sample preselection, however, reduces considerably the amount of data for the NBL estimation (Reimann et al., 2005). Due to the challenges in defining pristine areas in the test sites, mainly because of insufficient metadata accompanying samples, we chose not to preselect samples based on their quality.

Acknowledging the simplification adopted compared to the more sophisticated updated methods, we utilised all available data for constructing the CP plots of nitrates (Fig. 7a) and sulfates (Fig. 7b). As already explained regarding the CP plots of chlorides and TDS, we assume the extensive reference database embeds much of the information

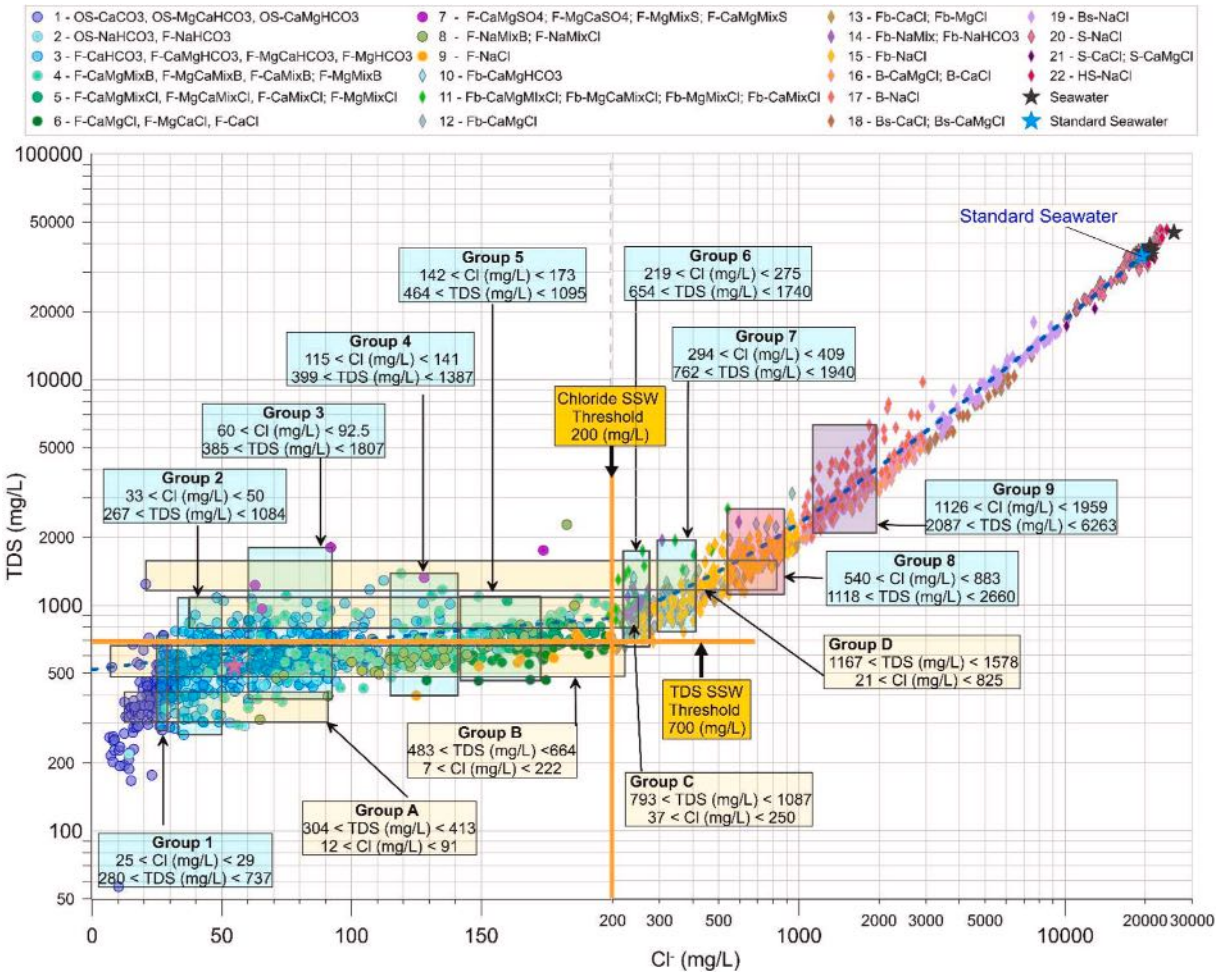

Fig. 6. TDS vs. chloride concentration (in mg/L). Data are distinguished according to the SFs. The x-axis is divided into two parts, the first with a linear scale covering the freshwater range (for 0 < Cl (mg/L) < 200) and the second with a logarithmic scale for 200 < Cl (mg/L) < 30000.

on the processes concerning nitrates and sulphates. By studying the cumulative frequencies of their concentrations without making assumptions about the underlying data, we could distinguish natural concentrations from those caused by a process that is likely common: human-induced contamination.

They CP plots show polymodal distributions. Each plot shows a first significant slope change between two primary groups (Group I-NO_3 and Group II-NO_3; Group I-SO_4 and Group II-SO_4). The skewness and p-values of the nitrate group's populations show that they are normally distributed, while Group I-SO4 population is log-normally distributed and Group II-SO4 population is normally distributed (Appendix A: Table A.3). We selected 13 mg/L as NBL for nitrates, corresponding to the value separating Group I-NO_3 and Group II-NO_3. The NBL for nitrates is close to 10 mg/L as suggested by Torres-Martínez et al. (2020) being generated by natural sources (natural fertilization, bacterial production, atmospheric deposition). The NBL for sulfates is set at the upper limit of Group I-SO4 (90 mg/L). Between this limit and the lower limit of Group II-SO_4 there is a gradual transition because of the overlapping of the two populations. The NBL of sulfates is close in the mean of the NBLs estimated by Lions et al. (2021).

Fig. 8 presents a crucial aspect of our research, showcasing the binary plots of nitrate (a, c) and sulfate (b, d) concentration vs Cl and TDS, respectively, in OS and F waters. These concentrations, when compared to the nitrate and sulfate NBLs, reveal a significant finding. Despite being expected to be the cleanest waters in pristine areas, OS waters are not immune to nitrates input, even if concentrations generally remain below 50 mg/L (EU drinking water standard; EU, 2020).

Nitrate and sulfate inputs partly affect also the F SFs. Only 4 % and 1 % of F waters exceed the EU drinking standards for nitrates and sulfates (250 mg/L), respectively. However, the concentrations of the two ions are not linearly correlated, as would be expected if they both came from fertilizers. The sulfate/nitrate ratio (in mg/L) varies from more than 1000 to 0.1. Note, for example, class 7 in Fig. 8 (F-CaMgSO4; F-MgCaSO4; F-MgMixS; F-CaMgMixS), for which very high concentrations of sulfates correspond to concentrations of nitrates even below the NBL. Given the various possible natural and human origins of sulfates, which are difficult to ascertain even considering $\delta^{34}S$ (Spoelstra et al., 2021) and that could affect the related NBL, we will primarily use nitrates to detail the categorization, supplementing it with the available data on corresponding sulfate concentrations.

The above considerations do not change the conclusions regarding the chloride SSW threshold. Even though they raise further questions about using TDS as an indicator of SSW, they also suggest that TDS, in the OS and F waters fields, may serve as an indicator of other groundwater salinization processes, different from SSW.

4.3. *Categorization of groundwater in coastal aquifers*

The final categorization of groundwater in coastal aquifers relies on the results described in pars 4.1 and 4.2., namely their chloride grouping (Fig. 4a and Fig. 6), the distribution of dominant and subordinate SFs in the Main Types (Table 4) and the additional information from Fig. 7 and Fig. 8. The categorization establishes Main Classes (MC), by splitting some of the Main Types and further divides them in Sub-Classes (SC),

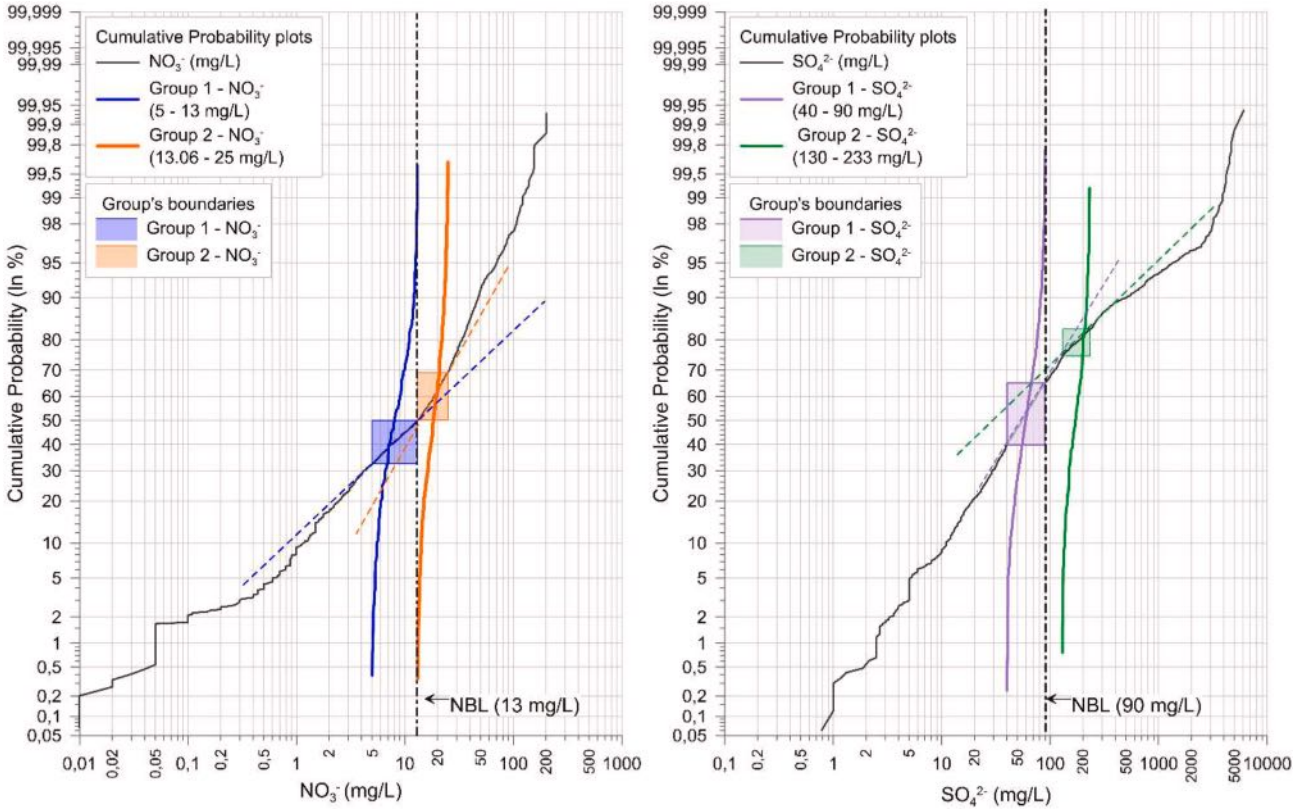

Fig. 7. CP plots of (a) nitrates and (b) sulfates, with indication of the two respective groups and CP plot of the related populations. Vertical bars outline the NBL ranges corresponding to the gradual transition between groups.

based on pollutant concentrations.

To define the sub-classes, we establish three water quality categories with different nitrates and sulfates limits: (a) $NO_3^- <$ NBL and $SO_4^{2-} <$ NBL, (b) NBL $< NO_3^-$ (mg/L) < 50 and $SO_4^{2-} <$ NBL, and (c) $NO_3^- > 50$ mg/L and $SO_4^{2-} < 250$ mg/L, which also consider the EU drinking water standards. The sub-classes apply to all samples with chlorides < 275 mg/L (so including some samples over the chloride SSW threshold). The samples with chlorides > 275 mg/L are not subject to partition in sub-classes.

Fig. 9 shows the limits of the MC and SC classes on the TDS-Cl relationship. Table A.4 (Appendix A) shows the statistical parameters concerning TDS, chlorides, nitrates and sulfates of the MCs. The SC limits cross each other because they are built based on different ranges of nitrates but often show similar TDS and chloride concentrations.

The Box-plots in Fig. 10 show the ranges of variation of TDS, chlorides, nitrates, and sulphates of the SCs. Data related to Fig. 10 are in Appendix A: Tables A.5a, A5b, A5c, and A5d, respectively.

The Main Class OS (Cl $\leq$ 30 mg/L; mean TDS = 397 mg/L; Appendix A: Table A.4) gathers all OS waters, which are the only groundwaters remaining under the TDS GWS threshold. The MC OS includes Group 1 waters (Fig. 6). The OS waters result from the progression of WRI processes on early infiltration waters without significantly changing chloride concentrations. Nevertheless, they are partially affected by anthropogenic inputs. Thus, based on nitrate and sulphate concentrations and according to the water quality categories previously defined, the MC OS splits into two sub-classes, OSa and OSb. The former comprises early infiltration waters of the recharge areas devoid of anthropogenic inputs. The latter includes OS waters, which exhibit signs of pollution. The mean concentrations of nitrates, sulfates and TDS increase from OSa to OSb (Fig. 10; Appendix A: Table A.5).

The broad F Main Type splits in two Main Classes: I-F (30 < Cl mg/L $\leq$ 93; mean TDS = 592 mg/L; Appendix A: Table A.4) and II-F (93 < Cl $\leq$ 200 mg/L; mean TDS = 692 mg/L; Appendix A: Table A.5).

The I-F MC includes the chloride Groups 2 and 3 (Fig. 6). Even if the mean TDS increases compared to the OS waters, some of the salinization facies characterising such main class (Fig. 9) are similar to those characterising the OS MC (F-CaHCO3, F-CaMgHCO3, F-MgCaHCO3, and F-NaHCO3. However, the appearance of Mix facies of B (bicarbonate) type, suggests small salt inputs. A few waters are of S (sulfate) type because of sulfate concentrations higher than 250 mg/L. The MC I-F waters show to be more evolved from the geochemical point of view compared to OS waters. The I-F class partitions in the I-Fa, I-Fb, and I-Fc Sub-Classes. They show similar mean chloride concentrations, but from I-Fa to I-Fc, the mean concentrations of nitrates and sulfate and the mean TDS increase (Fig. 10; Appendix A: Table A.5).

The MC II-F, which includes waters of Groups 3 and 4 (Fig. 6), shows a higher mean TDS compared to the MC I-F, thus evidencing a further progress of WRI compared to the I-F MC, including the solutions of salts. The Main Class II-F shows the predominance of Mix salinization facies, with subordinate -Cl facies. The latter indicates groundwater is subject to refreshing after having been salinised in previous periods (Appelo et al., 1990; Beekman, 1991). These findings also suggest that we are very close to the SSW threshold. The MC II-F splits into three Sub-Classes: the II-Fa, the II-Fb (gathering groundwater subject to anthropic inputs); and II-FC, showing the highest signs of pollution. The average nitrate, sulfate, and TDS concentration increases from II-Fa to II-Fc (Fig. 10; Appendix A: Table A.6). The sub-class II-Fc shows the highest mean values of nitrates and sulfates and the highest TDS within the F waters.

Groundwater samples with 200 < Cl (mg/L) $\leq$ 275 and mean TDS = 941 mg/L belong to the FS (Fresh-Saline) Main Class, which includes Group 6 (Fig. 6). This Main Class stays beyond the chloride threshold and mostly above the 700 mg/L TDS threshold. It represents the realm of the early onset of salinisation because of mixing with seawater and/or saline fluids. The few fresh calcium and magnesium bicarbonate, expected before the Cl threshold, transition to the Fb −MixCl and Cl facies

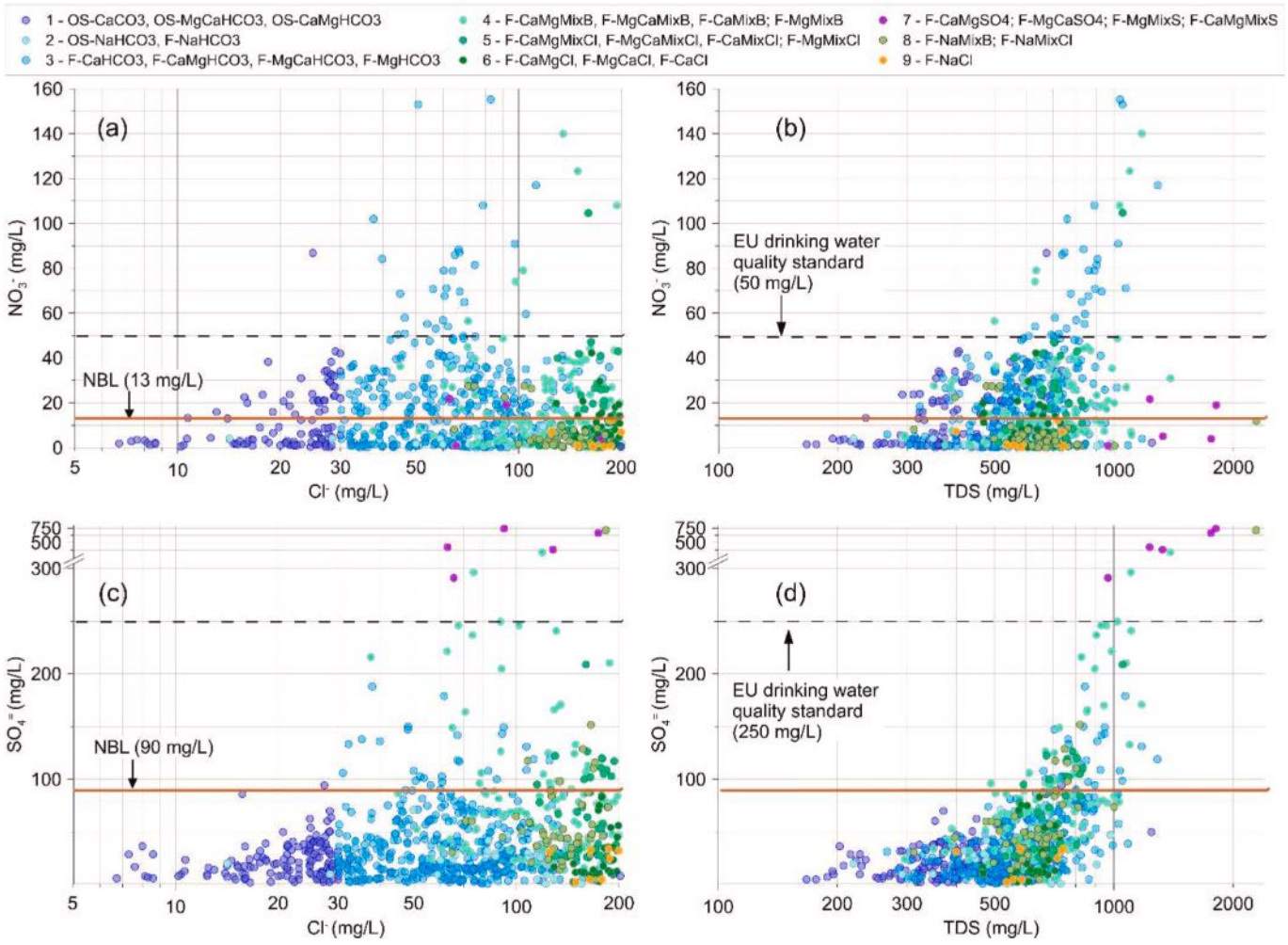

Fig. 8. Binary plots of nitrate (a) and sulfate (c) concentration vs Cl, and nitrate (b) and sulfate (d) vs TDS for groundwater with Cl < 200 mg/L. Data are distinguished per SF and compared to the NBLs and drinking water standards (EU, 2020).

because chloride increases in percentage compared to bicarbonates. According to the pollutant concentration ranges, the FS class partitions in the SCs FSa, FSb, and FSc: among the FS Sub-classes, the FSc shows the highest means of nitrates, sulfates, and TDS concentrations (Fig. 10; Appendix A: Table A.5).

The Main Class I-S (275 < Cl mg/L ≤ 1,000; mean TDS = 1,434 mg/L) includes waters of Groups 7 and 8 (Fig. 6). The class gathers waters belonging to the fresh-brackish (Fb) facies such as Fb-NaCl, Fb-CaMgCl, Fb-CaCl, Fb-MgCl and a few −MixCl, typical of SSW salinisation, which in most regions, notwithstanding the high salt contents, are used in agriculture. This MC encompasses waters at the initial salinisation stage subject to high geochemical disequilibrium. 10 % of samples overcome the 50 mg/L of nitrates.

The class II-S (1,000 < Cl (mg/L ≤ 3,000; mean TDS = 3,650 mg/L) includes Group 9 (Fig. 6). The class gathers brackish SFs such as B-NaCl, B-CaMgCl, B-CaCl, and B-MgCl, subject to progressive salinisation. The mixing with saline fluids justifies the high sulfate content, but the class still shows nitrate concentrations higher than 50 mg/L (21 % of samples).

Waters with 3,000 < Cl (mg/L ≤ 10,000 and mean TDS of 9,614 mg/L include all brackish-salt (Bs) SFs as Bs-NaCl, Bs-CaCl, and Bs-CaMgCl. They belong to the MC III-S. Nitrates exceeding 50 mg/L mark 13 % of samples, once again revealing the extent of the vertical migration of pollutants.

The last MC is the IV-S (Cl > 10,000 mg/L) with saline (S) and hypersaline (HS) ground waters, mean TDS of 34,188 mg/L and low concentrations of nitrates.

After the SSW chloride threshold all classes show deviations from the FW-SW mixing line, likely caused by the overlapping of various salinisation sources and triggered WRI processes. Fig. 11 synthesizes the previous considerations in a decision tree.

5. Discussion

The result regarding the salinisation threshold for SSW may seem considerably sharp, given the complexity of the aquifers considered. However, the consistency and high statistical significance of the DB and variety of the coastal aquifers' geological and hydrogeological settings highlight the threshold's potential value as a preliminary diagnostic tool for data evaluation for the concerned aquifers.

It is worth underlining that the study refers to data from waters that we can no longer consider "natural": coastal aquifers worldwide are subject to the highest demographic pressures and significant alterations that have moved groundwater away from an undisturbed condition. The threshold is determined using data referring to a few past decades, which partly cover the periods of significant growth of irrigated areas in the Mediterranean with a consequent increase in exploitation (European Commission, 2007) and the greatest alterations in quality observable today.

Our research, aimed at understanding the start of a precise process (mixing) and its effects on chlorides. Supposing that various sources of salinisation and different processes lead to varying increases in chloride

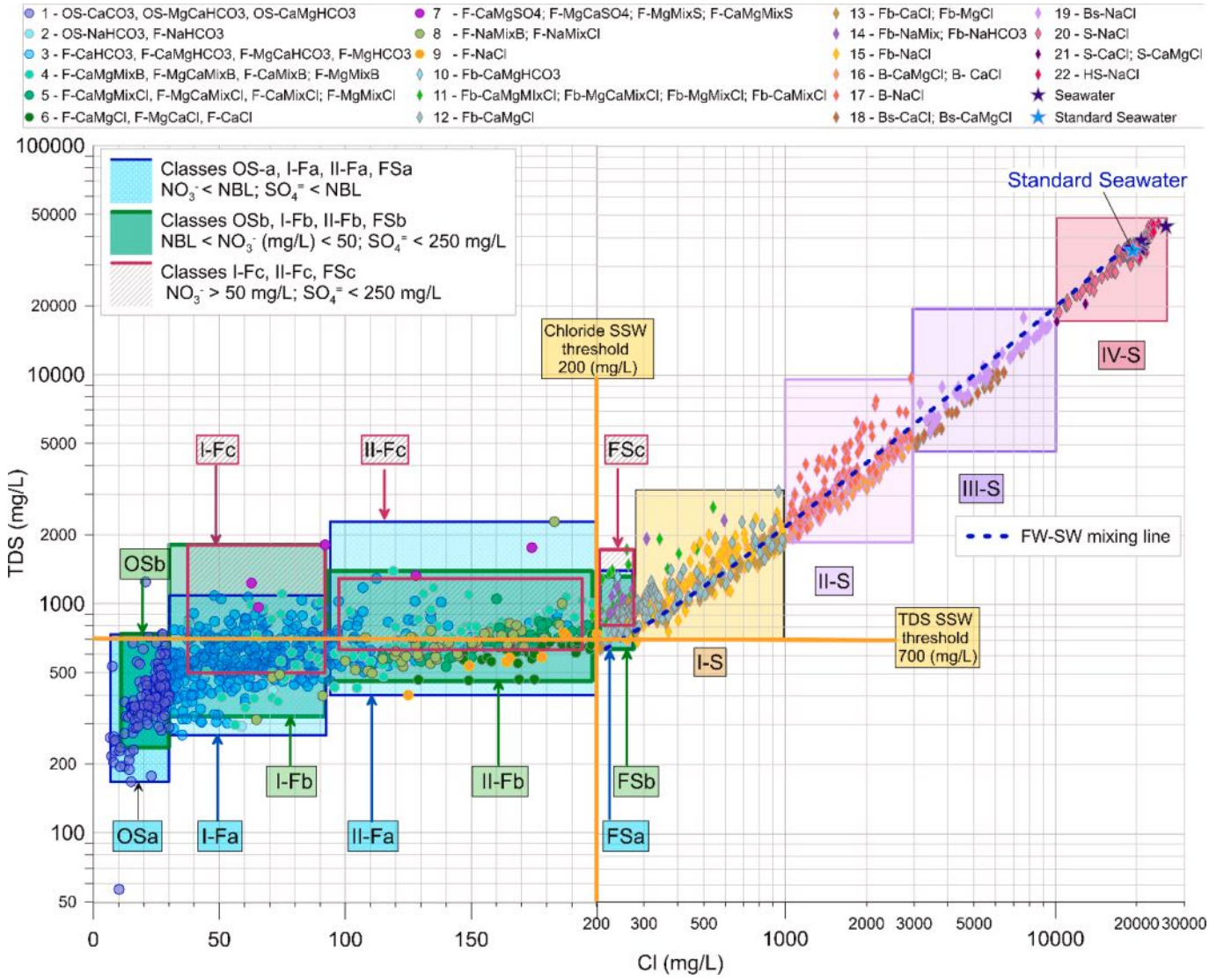

Fig. 9. Relationship between TDS vs. chloride concentration with limits of Main Classes and Sub-Classes. Data are distinguished according to the SF classification.

concentration trends, our aim was to distinguish the effects of mixing with present-day seawater from those caused by other sources, including human activities.

The results unequivocally demonstrate that a highly 'nonreactive' indicator of SSW is chloride. Other halogenides (F, B) form part of geochemical processes or are less generally applicable (Br). In contrast, the TDS SSW threshold fails to provide equivalent information. These findings warrant caution, particularly in the everyday use of TDS to differentiate fresh from salinised waters due to SSW. This caution also extends to EC due to the EC-TDS correlation. The EC of the solution is a complex function influenced by the rate of movement of charges in the potential field, which is, in turn, influenced by the migration speed of individual ions, charges and concentrations of ions, and interactions among individual ions. TDS and EC also reflect changes in hydrogenic carbon and geogenic conditions in the coastal basin or aquifer system unrelated to SSW. The unequal influence of different solutes on EC means that the same EC value can correspond to different water chemical compositions and TDS values at the point that TDS and EC show low correlation, especially if Cl $<$ 200 mg/L.

The caution in using the TDS SSW threshold also rests on the fact that freshwater pollution by non-chloride salts, wastewater and organic fertilizers, accompanied by triggered reactions, highly impacts the TDS values of freshwater. Wastewaters (which also add chlorides) and fertilizers cause nitrate pollution, which is a common problem of coastal aquifers. Nitrates (and their leaching affecting sulfate concentration), while still serving as 'per se' as unwanted pollutants, also indicate a far more concerning issue than seawater intrusion because of the extent of contaminant co-occurrence, like the 'chemical cocktails' of heavy metals and organic compounds (Kaushal et al., 2018) negatively affecting groundwater quality. Moreover, the recent recognition of lags in their transport in the unsaturated and saturated zone (Van Meter et al., 2016) might soon cause an unexpected increase in their concentration, notwithstanding the adoption of good practices, effectively reducing the fertilizer input in most countries in the last decades. While also of natural origin, the sulfate concentration must be noticed because agriculture accounts for about 50 per cent of the sulfur discharged into the environment yearly (Zak et al., 2021).

The categorization shows that the most nitrate-polluted groundwaters have chlorides close to the limit of 200 mg/L. They are close to the discharge areas, where they transfer the pollutant load to the mixing zone (the FS class shows high nitrate contents), enhancing their mobility at depth and their transfer to the sea. Nitrates are pervasive and their presence is recognized even in the salinised classes, showing their mobility within the whole groundwater body. Thus, most waters we define as "fresh" because they are under the SSW threshold of chlorides suffer from GWS.

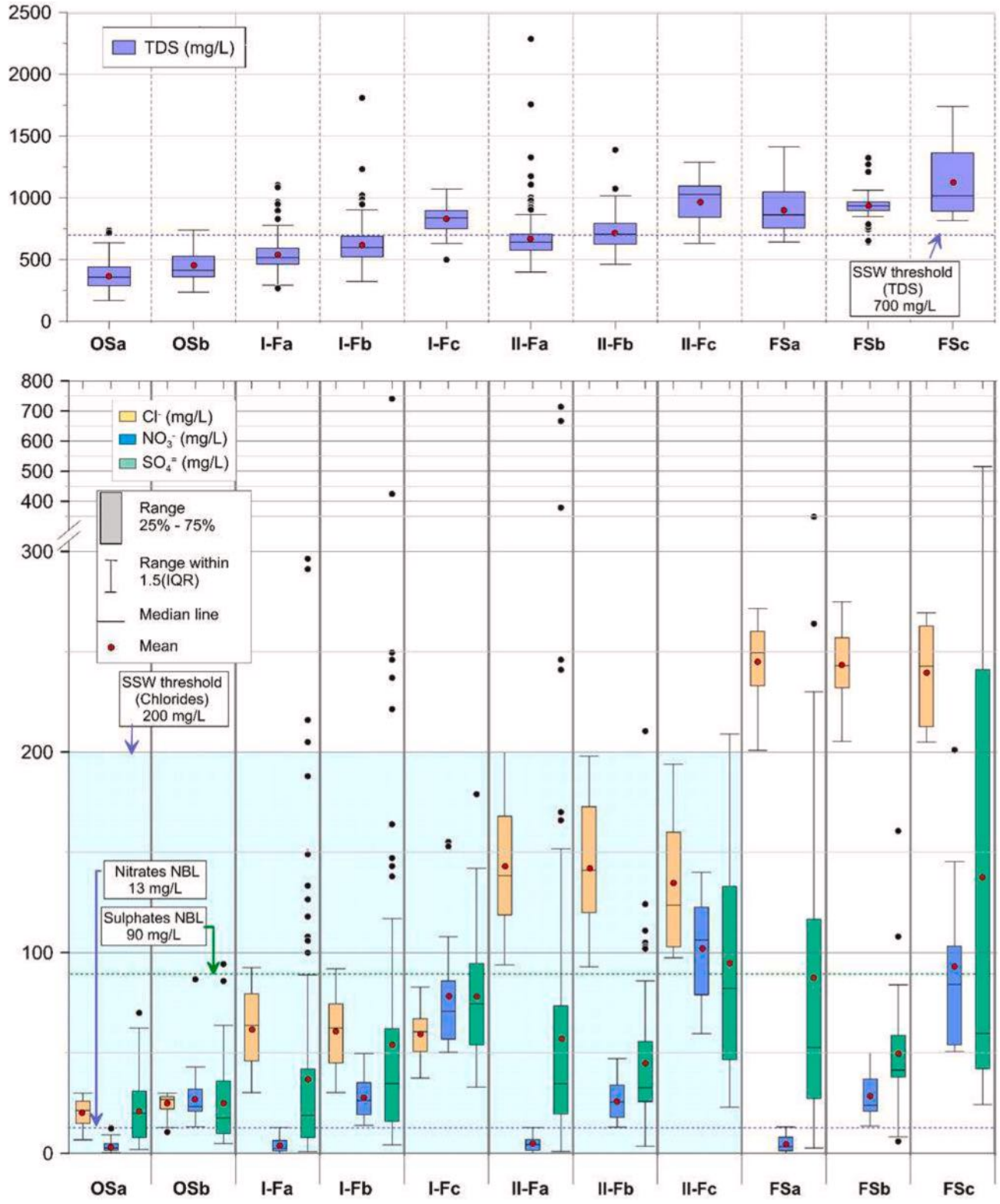

Fig. 10. Box plots referred to the Sub Classes of the Oligo-Saline and Fresh Main Classes (Cl < 200 mg/L), and Fresh-Saline MC (200 < Cl (mg/L) < 275).

The thresholds and categorization, set for preliminary screening to evaluate the groundwaters' main problems, have logical implications for the test sites.

Fig. 12 presents the DB samples divided per site, juxtaposed with the framework of MCs and SCs. It is important to note that each aquifer's lithology and hydrogeological structure, which are not to be underestimated, significantly condition the related sample's behavior in the TDS-Cl diagram. Despite this complexity, the diagram underscores the fact that before and over the SSW chloride threshold, the impact of pollution and different salinisation sources respectively contribute to differentiating the various sites. For samples below the chloride threshold, Fig. 13 shows binary plots of nitrate (a, c) and sulfate (b, d) concentration vs. Cl and TDS, respectively, for the OS and F waters of the test sites. Most samples of RHO and SAM show nitrate and sulfates under

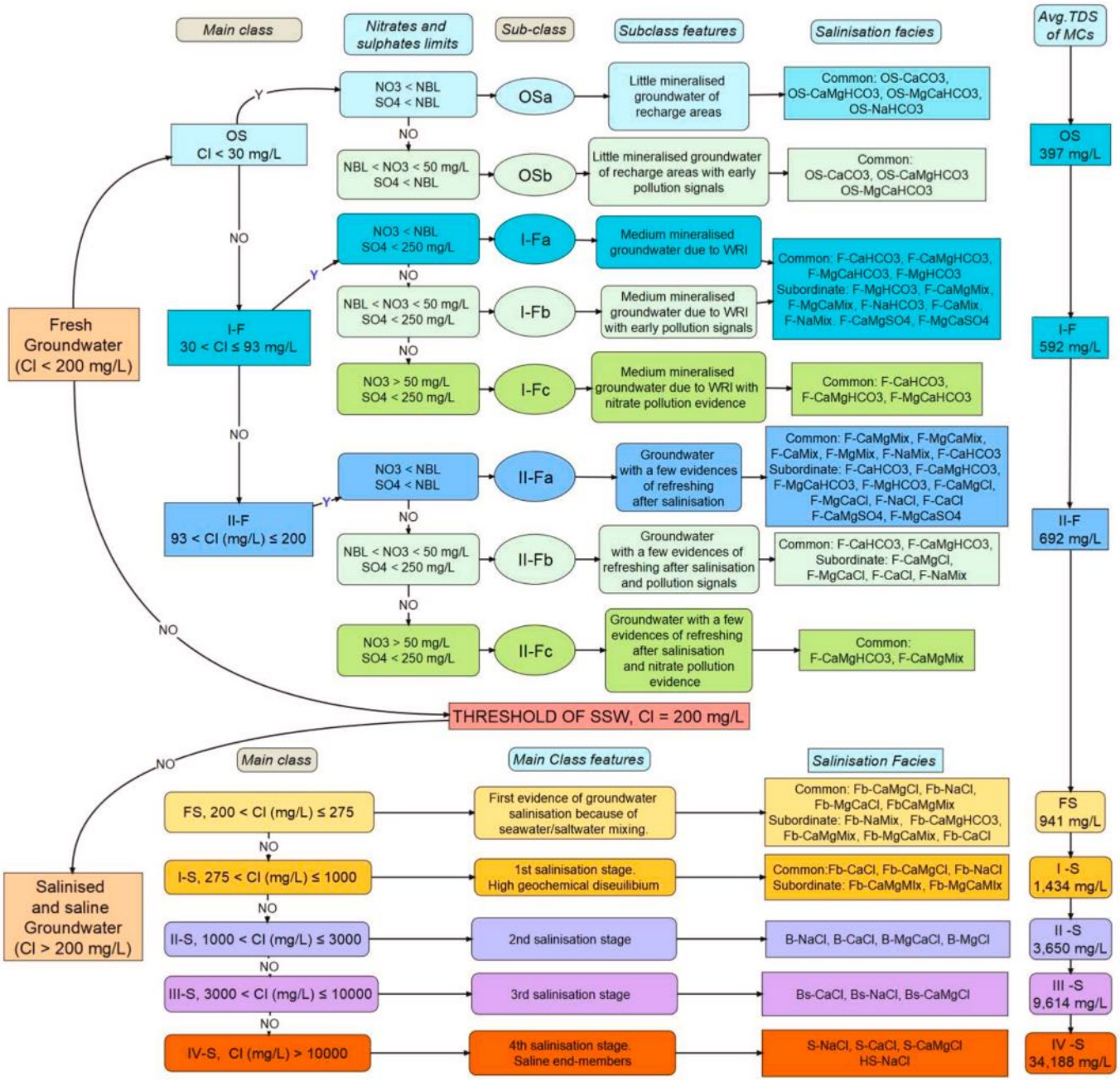

Fig. 11. Decision tree concerning the classification of fresh and salinised waters.

the respective NBLs. SAL and TAR samples in great proportion and a few samples of RHO and SAM exceed the NBLs remaining under the EU drinking standards (EU, 2020). SAL and TAR mostly exceed the EU drinking standard for nitrates, while only TAR shows high sulfate exceedances (note the truncated logarithmic y-axis) over the EU standard. Nitrate and sulfates concur in increasing the whole salinisation in freshwater especially for TAR and SAL.

Our analysis of samples over the chloride threshold has also provided significant preliminary insights. Fig. 14c, like Fig. 5c, demonstrates the dispersion of SFs when crossing the chloride threshold. SAL and SAM are dispersed around the FW-SW mixing line, while RHO primarily follows a divergent trend marked by the CaCl SF (Fig. 5a and Fig. 14a). BFC follows another trend, showing only NaCl or CaCl FSs with significant percentages of sulfates. TAR samples, with FSs variable from NaCl to CaCl with lower percentages of sulfates, do not follow any evident trend.

The preliminary screening thus unequivocally demonstrates the presence of GWS processes different from SSW in all areas, particularly where agriculture is intensive. These occurrences sound a general alarm for management, considering the already mentioned delay phenomena in nitrate transport, which might propose a worsening of nitrate concentrations in the future and suggest that focusing on sulfates from agriculture is urgently needed. Management must also change its perspective on using TDS (and EC) as SWI indicators.

The dispersion of samples over the chloride threshold suggests that many sources of salinisation exist, which demand immediate and purposeful studies and a focus on considering monitoring all the salinity spectrum to recognize the fresh (as needed for BFC) and saline endmembers. The data from the RHO, SAL, SAM and TAR aquifers (Table 1) paint a comprehensive picture of the salinity range. However, the BFC aquifer, with its consistently high chloride concentrations,

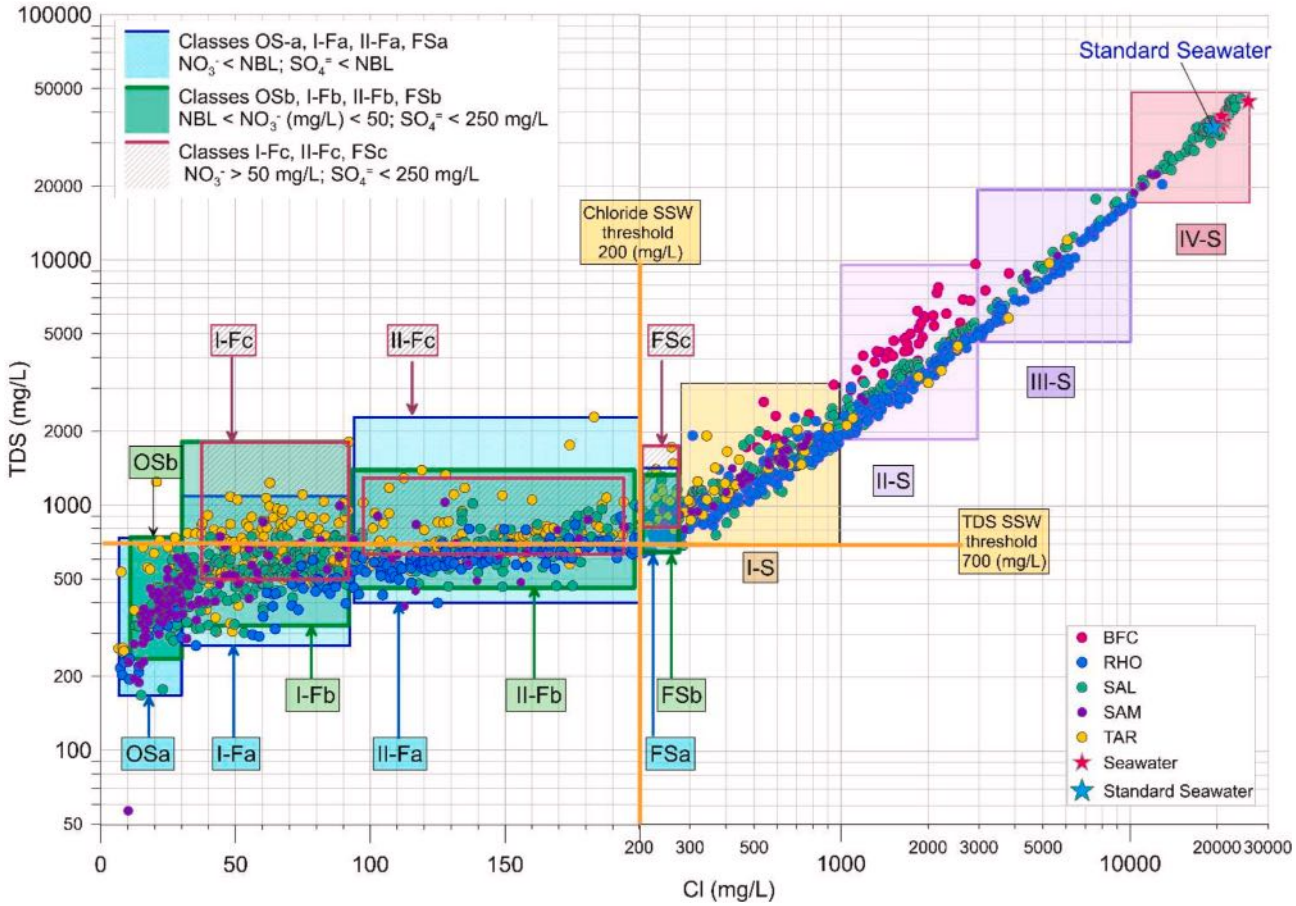

Fig. 12. Relationship between TDS vs. chloride concentration with limits of Main Classes and Sub-Classes. Data are distinguished according to the examined test sites.

presents a pressing issue.

This preliminary screening, while a crucial step, is just the beginning. It underscores the need to deepen our knowledge and ameliorate monitoring, actions that are desirable and imperative for understanding groundwater issues.

6. Conclusions

The availability of historical chemical data on groundwaters from coastal aquifers of the Mediterranean area with diverse features and spatial scales, combined with the high statistical significance of the DB data, and the comprehensive coverage of the salinity range elicited the emergence of 'signals' that likely would not have come to light from the individual datasets. Contrary to the prevailing belief in the public imagination and literature that seawater intrusion is the primary (if not unique) process causing groundwater salinisation in coastal aquifers, the experience and research findings demonstrate that such salinisation comes from various sources and that the direct attribution of groundwater salinisation to seawater intrusion may often be inaccurate. Thus, our focus was on establishing a salinisation threshold that could indicate the onset of this single phenomenon while helping to recognize the other causes of salinisation.

The DB processing began by considering chlorides and the major ions (to calculate the TDS). Chlorides and TDS are common seawater intrusion indicators available in most countries' historical groundwater chemical datasets.

The first contribution of our study is establishing the salinisation threshold because of seawater intrusion at 200 mg/L of chlorides by analyzing the chloride Cumulative Probability plot. Examining the SFs across the threshold and within the sample groups provides its validation. This finding has direct practical implications for the field, as it provides a clear benchmark for identifying and managing seawater intrusion. As the study areas include coastal basins north, east and south of the Mediterranean with climatic conditions encompassing arid to semi-arid conditions, the threshold can be considered a preliminary diagnostic tool for data evaluation of a general applicability in the Mediterranean region. Considering the diverse climatic, geological, and hydrogeological conditions on a global scale, the chosen threshold's significance may vary. However, incorporating substantial datasets from other regions has the potential to expand its relevance.

The CP plot of TDS cannot provide comparable information because chlorides behave as nonreactive tracers of seawater intrusion, and, on the contrary, TDS behaves as a reactive tracer given that its values derive from several overlapping and synergizing factors of groundwater salinisation. A practical consequence of the above issues is that TDS (but also EC), even maintaining its general diagnostic value regarding the control capacity about changes in groundwater saline content, should not be used as a standing-alone indicator of groundwater salinisation, especially if chlorides are lower than 200 mg/L. We must evaluate TDS and EC together with chloride concentrations and potential sources of salinisation from the human activities.

The second contribution concerns the evidence of two primary and linked issues that modify and broaden the concept of salinisation. The seawater's closeness to the aquifers generally leads to attributing fresh groundwater mineralisation to only seawater intrusion. The DB data processing results suggest groundwater management in the examined aquifers has more pressing problems than salinisation by seawater intrusion. If a predominant "natural salinisation" from mixing with

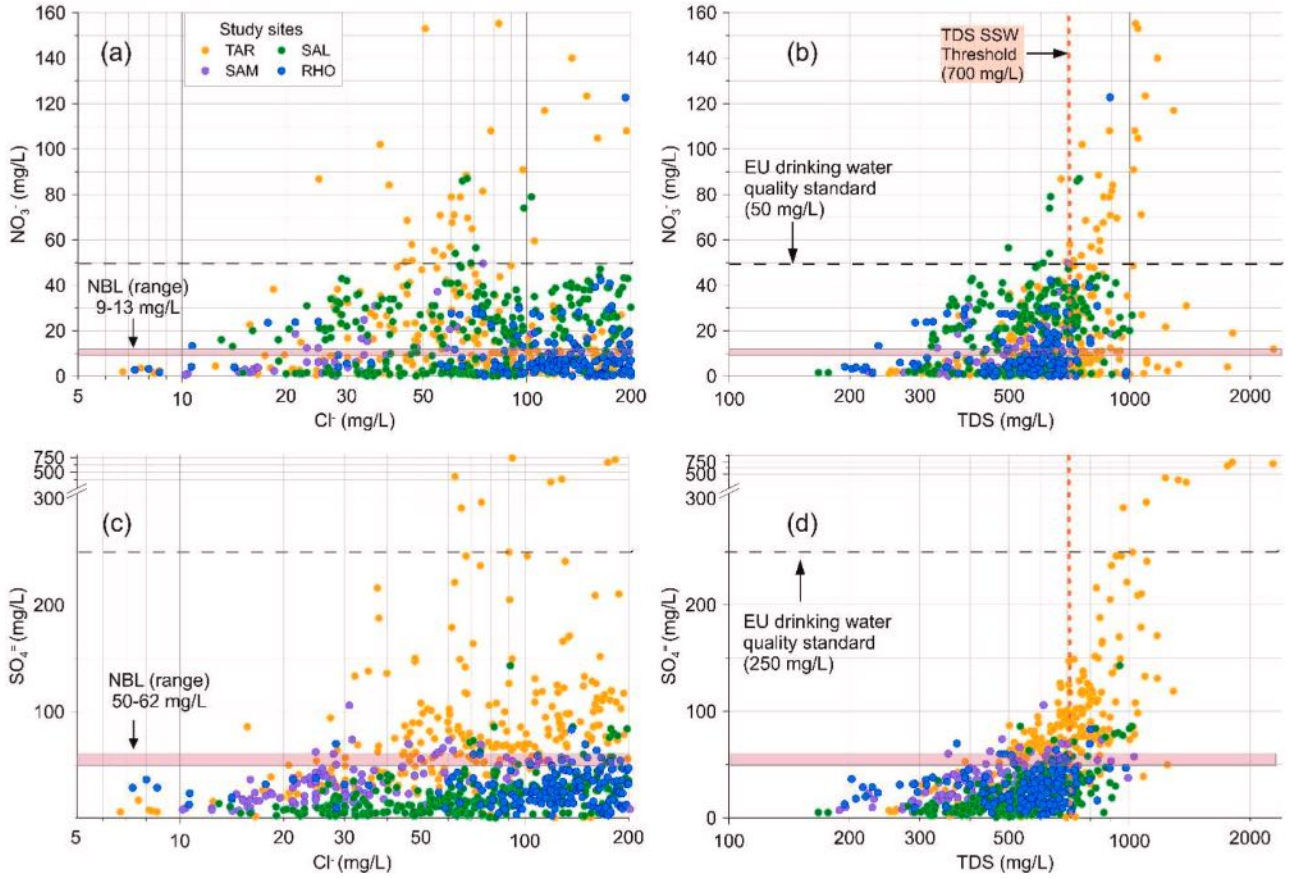

Fig. 13. Binary plots of nitrate (a, c) and sulfate (b, d) concentration vs Cl and TDS, respectively for the OS and F waters of the test sites.

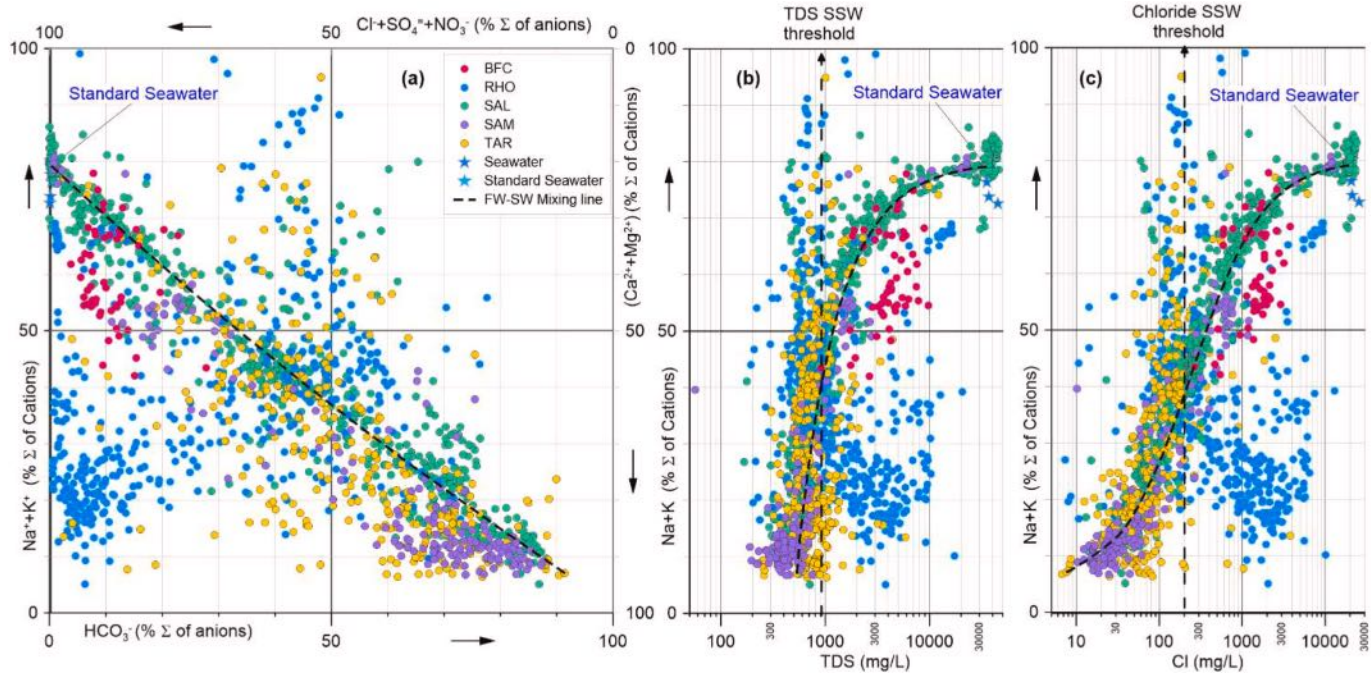

Fig. 14. Chebotarev diagram of all DB samples distinguished per test site; (b) Na + K (% sum of cations) vs. TDS (mg/L); (c) Na + K (% sum of cations) vs. chloride concentration (mg/L).

seawater or saltwater affects groundwater with Cl > 200 mg/L, the analysis revealed another type of salinisation within the limits of freshwater (with Cl < 200 mg/L) typically not coupled with a chloride input, which we can refer to as 'anthropic salinisation'.

The third key contribution is the proposal of a new method involving a simple decision tree to categorize groundwater in coastal aquifers. The

incorporation of data from other coastal aquifers might change the limits of some classes and subclasses, but the statistical significance of the DB makes the value of the chloride threshold sufficiently reliable to be applied worldwide as preliminary screening tool. The method for establishing the chloride threshold can be used in general, requiring only a significant amount of historical groundwater chemical analyses related to major ions and nitrates. Although the need for more advanced analyses and parameters limits our understanding of the chemical processes within each class, the advantage of this method is that it is easy to apply in situations where data is scarce, which is often the case with both historical data and current monitoring in many countries.

The fourth key contribution of this research is the identification, after the SSW threshold, of emergent signals of diverse salinisation processes beyond simple seawater mixing. This discovery was made possible due to the comprehensive coverage of the entire spectrum of groundwater salinity in coastal aquifers. The complex nature of the facies and trends of samples with chlorides higher than 200 mg/L strongly indicates the existence of multiple overlapping sources of salinisation, which demands further investigation in future research.

The threshold and the categorization hold significant relevance, considering the cascade effects their application may trigger on groundwater management.

A valuable tool for distinguishing the processes and sources of groundwater salinisation significantly enhances the integrated management of coastal aquifers by facilitating the recognition of FW salinisation sources, and the early detection of the onset of SSW.

This study also highlights the importance of multi-site studies and establishing a database adhering to validated quality standards across various study areas. The multi-site perspective and analysis indicated common trends of hydrochemical evolution that can be generalized such as salinisation thresholds. At the same time, compared to the background of generalized evolution, site-specific differences become visible and apparent.

Concerning FW salinisation sources, the role of scientists and policymakers in addressing the implication of such GWS on the threshold established by current laws for distributing drinking water, is crucial. For routine purposes, we need more than simple criteria based on coupling information about chloride concentrations less than 250 mg/L, EC less than 2,500 mS/cm, and nitrates less than 50 mg/L. In addition, considering the increased frequency of sulfate increase findings, even if their source may be natural, we should set limits for them. Such indicators' single and concurrent increase should be assumed as a warning signal, even when their concentrations are under the limits. The interpretation of the results produced by the proposed classification should be considered jointly with local conditions, such as the hydrology/hydrogeology and the land use, to properly conclude to the final assessment. In such cases, the risk should be evaluated by thoroughly assessing the whole water quality and monitoring it more frequently. The control of the anthropogenic inputs should avoid implementing ineffective mitigation measures of groundwater mineralization, mistaken for seawater intrusion, often based on misleading information from TDS.

As to the SSW chloride threshold, the proposed methodology can be incorporated into integrated water resource management frameworks. This way, managers can adopt a more proactive and preventive approach to groundwater management. Policymakers can use the threshold to establish water quality standards, guide land use planning, and allocate resources for groundwater protection and remediation.

Advances in monitoring technology, integration with other indicators, and community engagement can enhance the reliability and utility of the chloride threshold. As part of a comprehensive strategy for managing coastal aquifers, this threshold can play a crucial role in preserving groundwater quality and ensuring the sustainability of vital water resources.

CRediT authorship contribution statement

M.D. Fidelibus: Writing – review & editing, Writing – original draft, Validation, Supervision, Methodology, Funding acquisition, Formal analysis, Conceptualization. **G. Balacco:** Writing – review & editing, Writing – original draft, Validation, Resources, Methodology, Investigation, Conceptualization. **M.R. Alfio:** Writing – review & editing, Visualization, Resources, Investigation, Data curation. **M. Arfaoui:** Investigation, Data curation. **D. Bassukas:** Writing – review & editing, Resources, Investigation, Data curation. **C. Güler:** Writing – review & editing, Validation, Methodology, Investigation, Funding acquisition, Data curation, Conceptualization. **F. Hamzaoui-Azaza:** Writing – review & editing, Investigation, Funding acquisition, Data curation. **C. Külls:** Writing – review & editing, Validation, Methodology, Investigation, Data curation, Conceptualization. **A. Panagopoulos:** Writing – review & editing, Visualization, Validation, Resources, Investigation, Conceptualization. **A. Parisi:** Writing – review & editing, Visualization, Validation, Resources, Investigation, Data curation. **E. Sachsamanoglou:** Writing – review & editing, Visualization, Validation, Resources, Investigation, Data curation. **E. Tziritis:** Writing – review & editing, Writing – original draft, Validation, Resources, Project administration, Methodology, Investigation, Data curation, Conceptualization.

Declaration of competing interest

The authors declare that they have no known competing financial interests or personal relationships that could have appeared to influence the work reported in this paper.

Acknowledgements

This research is conducted in the context of MEDSAL Project© (www.medsal.eu), which is part of the PRIMA Programme supported by the European Union's Horizon 2020 Research and Innovation Programme and funded by the national funding agencies of GSRT, Greece (grant number 2018–7); MHESR and BMBF, Germany (grant number 01DH19027); MIUR, Italy (grant number: 1421); Tunisia (grant number 2018–12); TÜBITAK, Turkey (grant number: 118Y366).

Appendix A. Supplementary data

Supplementary data to this article can be found online at https://doi.org/10.1016/j.jhydrol.2025.132775.

Data availability

Data will be made available on request.

References

Appelo, C.A.J., Beekman, H.E., Griffioen, J., Willemsen, A., 1990. Geochemical calculation and observations on salt water intrusions. II. Validation of a geochemical model with laboratory experiments. J. Hydrol. 120 (1–4), 225–250. https://doi.org/10.1016/0022-1694(90)90151-M.

Appelo, C.A.J., Geirnaert, W., 1983. Processes accompanying the intrusion of saltwater. In De Breuck W. (Ed.) Hydrogeology of salt water intrusion: a selection of SWIM papers. International contributions to hydrogeology, 11, ISSN 0936-3912, 291-303.

Appelo, C.A.J., Postma, D., 2005. Geochemistry, groundwater and pollution, 2nd Ed.,. CRC Press.

Appelo, C.A.J., Willemsen, A., 1987. Geochemical calculations and observations on saltwater intrusions, I. A combined geochemical/mixing cell model. J. Hydrol. 94, 313–330. https://doi.org/10.1016/0022-1694(87)90058-8.

Balacco, G., Alfio, M.R., Parisi, A., Panagopoulos, A., Fidelibus, M.D., 2022. Application of short time series analysis for the hydrodynamic characterization of a coastal karst aquifer: the Salento aquifer (Southern Italy). Journal of Hydroinformatics 24 (2), 420–443. https://doi.org/10.2166/hydro.2022.135.

Beekman, H.E., 1991. Ion chromatography of fresh- and seawater intrusion. Multicomponent dispersive and diffusive transport in groundwater. Vrije Universiteit, Amsterdam. PhD thesis ISBN: 9090047093, 9789090047096.

Buvaneshwari, S., Riotte, J., Sekhar, M., et al., 2020. Potash fertilizer promotes incipient salinization in groundwater irrigated semi-arid agriculture. Sci. Rep. 10, 3691. https://doi.org/10.1038/s41598-020-60365-z.

Calaforra, J. M. (ed), 2005. The Main Coastal Karstic Aquifers of Southern Europe : A Contribution by Members of the COST-621 Action 'Groundwater Management of Coastal Karstic Aquifers', EU Publications Office (OPOCE), ISBN/ISSN: 92-894-6413-5, EUR: 20911, http://bookshop.europa.eu/uri?target=EUB:NOTICE:KINA20911:EN:HTML.

Calaforra, J.M., Ballarin, L., Ginés, J., Perleros, V., Tiniakos, L., 2005. W.G.1, Characterization of coastal karstic aquifer. In: Tulipano L. et al. (Eds.), COST Action 621. "Groundwater management of coastal karstic aquifers". Final report 23-49. COST Office http://www.cost.eu/media/publications/05-12-Groundwater-Management-of-Coastal-Karstic-Aquifers-Final-Report.

Chachadi, A.G., Lobo-Ferreira, J.P., 2001. Sea water intrusion vulnerability mapping of aquifers using GALDIT method. In COASTIN, A Coastal Policy Research Newsletter 4, 7–9.

Chebotarev, I.I., 1955. Metamorphism of natural waters in the crust of weathering - 2, 8 (3), 137–170. https://doi.org/10.1016/0016-7037(55)90010-7.

Colombani, N., Osti, A., Volta, G., Mastrocicco, M., 2016. Impact of climate change on salinization of coastal water resources. Water Resour. Manage. 30 (7), 2483–2496. https://doi.org/10.1007/s11269-016-1292-z.

Cook, B.I., Anchukaitis, K.J., Touchan, R., Meko, D.M., Cook, E.R., 2016. Spatiotemporal drought variability in the Mediterranean over the last 900 years. J. Geophys. Res.: Atmos. 121, 2060–2074. https://doi.org/10.1002/2015JD023929.

Cotecchia, V. 1977. Studi e ricerche sulle acque sotterranee e sull'intrusione marina in Puglia (Penisola Salentina), Quaderno n. 20 dell'Istituto di Ricerca sulle Acque del C. N.R., Roma. (in Italian).

Cotecchia, V., 2017. Area idrogeologica del salento. In: Memorie Descrittive Della Carta Geologica d'Italia ISPRA—Istituto Superiore per la Protezione e la Ricerca Ambientale: Rome Italy, pp. 312–442 in Italian.

Demirel, Z., 2004. The history and evaluation of saltwater intrusion into a coastal aquifer in Mersin. Turkey. J Environ Man 70 (3), 275–282. https://doi.org/10.1016/j.jenvman.2003.12.007.

Demirel, Z., Güler, C., 2006. Hydrogeochemical evolution of groundwater in a Mediterranean coastal aquifer, Mersin-Erdemli basin (Turkey). Environ Geol 49, 477–487. https://doi.org/10.1007/s00254-005-0114-z.

Edmunds, W.M., Shand, P., Hart, P., Ward, R.S., 2003. The natural (baseline) quality of groundwater: a UK pilot study. Sci. Total Envir. 310 (1–3), 25–35. https://doi.org/10.1016/S0048-9697(02)00620-4.

EEA, European Environment Agency (2024) Glossary, .

EPA, Environmental Protection Agency (2024) Safe Drinking Water Act (SDWA), Secondary Drinking Water Standards: Guidance for Nuisance Chemicals. https://www.epa.gov/sdwa/secondary-drinking-water-standards-guidance-nuisance-chemicals.

European Commission: Directorate-General for Environment, 2007. Mediterranean groundwater report : technical report on groundwater management in the Mediterranean and the water framework directive. Directorate-General for the Environment. https://op.europa.eu/en/publication-detail/-/publication/12eba428-48f3-406f-a8eb-819ace7fcee3.

European Union (EU) (2020) Directive (EU) 2020/2184 of the European Parliament and of the Council of 16 December 2020 on the quality of water intended for human consumption. https://eur-lex.europa.eu/legal-content/EN/TXT/PDF/?uri=CELEX:32020L2184.

Fidelibus, M.D., Pulido-Bosch, A., 2019. Groundwater temperature as an indicator of the vulnerability of karst coastal aquifers. Geosciences 9 (1), 23. https://doi.org/10.3390/geosciences9010023.

Galazoulas, E., Petalas, C., Tsihrintzis, V., 2011. Evaluation of multivariate statistical methods for the identification of groundwater facies, in a multilayered coastal aquifer. In: Lambrakis, N., Stournaras, G., Katsanou, K. (Eds.), Advances in the Research of Aquatic Environment. Environmental Earth Sciences. Springer, Berlin, Heidelberg, 10.1007/978-3-642-19902-8_37.

García, A., Maisonnave, R., Massobrio, M., Iorio, A., 2012. Field-scale evaluation of water fluxes and manure solution leaching in feedlot pen soils. J. Environ. Qual. 41 (5), 1591–1599. https://doi.org/10.2134/jeq2011.0320.

Gemitzi, A., 2012. Evaluating the anthropogenic impacts on groundwaters; a methodology based on the determination of natural background levels and threshold values. Environ. Earth Sci. 67, 2223–2237. https://doi.org/10.1007/s12665-012-1664-5.

Giménez, E., Morell, I., 1997. Hydrogeochemical analysis of salinization processes in the coastal aquifer of Oropesa (Castellón, Spain). Environ. Geol. 29, 118–131. https://doi.org/10.1007/s002540050110.

Giménez-Forcada, E., 2010. Dynamic of seawater interface using hydrochemical facies evolution diagram. Groundwater 48 (2), 212–216. https://doi.org/10.1111/j.1745-6584.2009.00649.x.

Giménez-Forcada, E., 2014. Space/time development of seawater intrusion, a study case in Vinaroz coastal plain (Eastern Spain) using HFE-diagram, and spatial distribution of hydrochemical facies. J. Hydrol. 517, 617–627. https://doi.org/10.1016/j.jhydrol.2014.05.056.

Giménez-Forcada, E., Sánchez San Román, F.J., 2015. An excel macro to plot the HFE-diagram to identify sea water intrusion phases. Groundwater 53 (5), 819–824. https://doi.org/10.1111/gwat.12280.

Güler, C., Kurt, M.A., Alpaslan, M., Akbulut, C., 2012. Assessment of the impact of anthropogenic activities on the groundwater hydrology and chemistry in Tarsus coastal plain (Mersin, SE Turkey) using fuzzy clustering, multivariate statistics and GIS techniques. Journal of Hydrology 414–415, 435–451. https://doi.org/10.1016/j.jhydrol.2011.11.021.

Hamzaoui-Azaza, F., Ameur, M., Chaouch, R., et al., 2020. Assessment of groundwater quality based on GIS and geochemical methods: coastal aquifer of Bouficha (North-Eastern Tunisia). J Coast Conserv 24, 45. https://doi.org/10.1007/s11852-020-00762-8.

Howard, K.W.F., Lloyd, J.W., 1983. Major ion characterization of coastal saline ground waters. Groundwater 21, 429–437. https://doi.org/10.1111/j.1745-6584.1983.tb00744.x.

John, Z., Krivy, M., 1965. Explanatory note of the geological map of Bouficha. ONM 11–72.

Kallioras, A., Pliakas, F., Diamantis, I., 2006. Conceptual model of a coastal aquifer system in northern Greece and assessment of saline vulnerability due to seawater intrusion conditions. J Environ Geol 51 (3), 349–361. https://doi.org/10.1007/s00254-006-0331-0.

Kaushal, S.S., Likens, G.E., Pace, M.L., et al., 2019. Novel 'chemical cocktails' in inland waters are a consequence of the freshwater salinization syndrome. Phil. Trans. R. Soc. B 374, 20180017. https://doi.org/10.1098/rstb.2018.0017.

Kaushal, S.S., Likens, G.E., Pace, M.L., et al., 2021. Freshwater salinization syndrome: from emerging global problem to managing risks. Biogeochemistry 154, 255–292. https://doi.org/10.1007/s10533-021-00784-w.

Leduc, C., Pulido-Bosch, A., Remini, B., Massuel, S., 2016. Changes in Mediterranean groundwater resources. In The Mediterranean Region under Climate Change, Sub-Chapter 2.3.5., 327-333, IRD, ISBN: 978-2-7099-2219-7.

Lepeltier, C., 1969. A simplified treatment of geochemical data by graphical representation. Econ. Geol. 64, 538–550. https://doi.org/10.2113/gsecongeo.64.5.538.

Limpert, E., Stahel, W.A., Abbt, M., 2001. Log-normal Distributions across the Sciences: Keys and Clues: On the charms of statistics, and how mechanical models resembling gambling machines offer a link to a handy way to characterize log-normal distributions, which can provide deeper insight into variability and probability—normal or log-normal: That is the question. Biosci. 51 (5), 341–352. https://doi.org/10.1641/0006-3568(2001)051[0341:LNDATS]2.0.CO;2.

Lions, J., Malcuit, E., Gourcy, L., et al., 2021. Proposing a common methodology to calculate the natural concentration of dissolved elements based on lithological/geological water families taking into account possible anthropogenic influences. Deliverable 3.3, GeoEra Groundwater project HOVER. https://repository.europe-geology.eu/egdidocs/hover/hover_33_statistical_data_treatment_backgroundlev.pdf.

Lloyd, W.J., Heathcote, A.J., 1985. Natural inorganic chemistry in relation to groundwater. Claredon Press, Oxford, p. 250.

Masciale, R., Amalfitano, S., Frollini, E., et al., 2021. Assessing natural background levels in the groundwater bodies of the apulia region (Southern Italy). Water 13 (7), 958. https://doi.org/10.3390/w13070958.

Mastrocicco, M., Colombani, N., 2021. The issue of groundwater salinization in coastal areas of the mediterranean region: a review. Water 13 (1), 90. https://doi.org/10.3390/w13010090.

Mountrakis, D., Kilias, A., Vavliakis, E., Psilovikos, A., Thomaidoy, E., 2003. Neotectonic map of Samos Island (Aegean Sea, Greece): implication of geographical information systems in the geological mapping. Proceed. 4th European Congress on Regional Geoscientific Cartography and Information Systems, June 2003, Bologna, Italy, Vol. 1: 11-13.

Müller. D., Blum, A., Hart, A., Hookey, J., Kunkel, R., Scheidleder, A., et al., 2006. Final proposal of a methodology to set up groundwater threshold values in Europe. www.wfd-bridge.net2006.

Milnes, E., Renard, P., 2004. The problem of salt recycling and seawater intrusion in coastal irrigated plains: an example from the Kiti aquifer (Southern Cyprus). J. Hydrol. 288 (3–4), 327–343. https://doi.org/10.1016/j.jhydrol.2003.10.010.

Panno, S.V., Kelly, W.R., Martinsek, A.T., Hackley, K.C., 2006. Estimating background and threshold nitrate concentrations using probability graphs. Groundwater 44, 697–709. https://doi.org/10.1111/j.1745-6584.2006.00240.x.

Parkhurst, D.L., Appelo, C.A.J., 2013. Description of input and examples for PHREEQC version 3—A computer program for speciation, batch-reaction, one-dimensional transport, and inverse geochemical calculations: U.S. Geological Survey Techniques and Methods, book 6, chap. A43, 497 p., available only at https://pubs.usgs.gov/tm/06/a43/.

Petalas, C., Diamantis, I., 1999. Origin and distribution of saline groundwaters in the Miocene aquifer system in coastal Rhodope area, Thrace. NE Greece. Hydrogeol J 7, 305–316. https://doi.org/10.1007/s100400050204.

Pulido-Velazquez, D., Baena-Ruiz, L., Fernandes, J., Arnó, G., Hinsby, K., Voutchkova, D. D., Hansen, B., Retike, I., Bikše, J., Collados-Lara, A.J., Camps, V., Morel, I., Grima-Olmedo, J., Luque-Espinar, J.A., 2022. Assessment of chloride natural background levels by applying statistical approaches. Analyses of European coastal aquifers in different environments. Marine Pollution Bulletin 174, 113303. https://doi.org/10.1016/J.MARPOLBUL.2021.113303.

Rahman, A., Mondal, N.C., Tiwari, K.K., 2021. Anthropogenic nitrate in groundwater and its health risks in the view of background concentration in a semi arid area of Rajasthan. India. Sci. Rep. 11, 9279. https://doi.org/10.1038/s41598-021-88600-1.

Reimann, C., Filzmoser, P., 2000. Normal and lognormal data distribution in geochemistry: death of a myth. Consequences for the statistical treatment of geochemical and environmental data. Envir. Geol. 39, 1001–1014. https://doi.org/10.1007/s002549900081.

Reimann, C., Filzmoser, P., Garrett, R.G., 2005. Background and threshold: critical comparison of methods of determination. Sci. Total Envir. 346 (1–3), 1–16. https://doi.org/10.1016/j.scitotenv.2004.11.023.

Revelle, R., 1941. Criteria for recognition of seawater in ground water. Trans. Am. Geophys. Union 22, 593–597. https://doi.org/10.1029/TR022i003p00593.

Sajil Kumar, P.J., 2017. Grounding a natural background level for fluoride in a potentially contaminated crystalline aquifer in south India. Environ. Sci. Pollut. Res. 24, 26623–26633. https://doi.org/10.1007/s11356-017-0239-0.

Sanford, R.F., Pierson, C.T., Crovelli, R.A., 1993. An objective replacement method for censored geochemical data. Math. Geol. 25, 59–80. https://doi.org/10.1007/BF00890676.

Seh-Chang, P., Seong-Taek, Y., Gi-Tak, C., In-Sik, Y., Kwang-Sub, S., Chul-Ho, H., Sang-Kyu, L., 2005. Regional hydrochemical study on salinization of coastal aquifers, western coastal area of South Korea. J. Hydrol. 313 (3–4), 182–194. https://doi.org/10.1016/j.jhydrol.2005.03.001.

Sinclair, A.J., 1976. Applications of probability graphs in mineral exploration, special volume No. 4. The Association of Exploration Geochemists, Richmond Printers LTD., Canada, p. 95.

Sinclair, A.J., 1974. Selection of threshold values in geochemical data using probability graphs. J. Geoch. Expl. 3 (2), 129–149. https://www.sciencedirect.com/science/article/abs/pii/0375674274900302.

Smolders, A.J.P., Lucassen, E.C.H.E.T., Bobbink, R., Roelofs, J.G.M., Lamers, L.P.M., 2010. How nitrate leaching from agricultural lands provokes phosphate eutrophication in groundwater fed wetlands: the sulphur bridge. Biogeochemistry 98, 1–7. https://doi.org/10.1007/s10533-009-9387-8.

Spoelstra, J., Leal, K.A., Senger, N.D., Schiff, S.L., Post, R., 2021. Isotopic characterization of sulfate in a shallow aquifer impacted by agricultural fertilizer. Groundwater 59, 658–670. https://doi.org/10.1111/gwat.13093.

Stamatakis, M., Tziritis, E., Evelpidou, N., 2009. The geochemistry of boron-rich groundwater in Karlovassi Basin, Samos Island. Greece. Central European Journal of Geosciences 1 (2), 207–218.

Stuyfzand, P.J., 1986. A new hydrochemical classification of water types: principles and application to the coastal dunes aquifer system of the Netherlands. 9th Salt Water Intrusion Meeting, Delft, 1986. http://swim-site.nl/pdf/swim09/swim09_Stuyfzand.pdf.

Tellam, J.H., Lloyd, J.W., Walters, M., 1986. The morphology of a saline groundwater body: Its investigation, description and possible explanation. J. Hydrol. 83 (1–2), 1–21. https://doi.org/10.1016/0022-1694(86)90179-4.

Tennant, C.B., White, M.L., 1959. Study of the distribution of some geochemical data. Econ. Geol. 54 (7), 1281–1290. https://doi.org/10.2113/gsecongeo.54.7.1281.

Torres-Martínez, J.A., Morab, A., Knappett, P.S.K., Ornelas-Soto, N., Mahlknecht, J., 2020. Tracking nitrate and sulfate sources in groundwater of an urbanized valley using a multi-tracer approach combined with a Bayesian isotope mixing model. Water Res. 182 (1), 115962. https://doi.org/10.1016/j.watres.2020.115962.

Tóth, J., 1963. A theoretical analysis of groundwater flow in small drainage basins. Journal of Geophysical Research 68, 4795–4812. https://doi.org/10.1029/JZ068i016p04795.

Tulipano, L., Fidelibus, M.D., Panagopoulos, A. (Eds), 2005. COST ACTION 621"Groundwater management of coastal karstic aquifers", Final Report, vol. EUR 21366, p. 1-363, Off. For Official Publ. of the European Commission, ISBN: 92-898-0015-1. http://www.cost.eu/media/publications/05-12-Groundwater-Management-of-Coastal-Karstic-Aquifers-Final-Report.

Tziritis, E., Sachsamanoglou, E., Aschonitis, V., 2023. Assessing groundwater evolution with a combined approach of hydrogeochemical modelling and data analysis: application to the rhodope coastal aquifer (NE Greece). Water 15 (2), 230. https://doi.org/10.3390/w15020230.

Van Meter, K.J., Basu, N.B., Veenstra, J.J., Burras, C.L., 2016. The nitrogen legacy: emerging evidence of nitrogen accumulation in anthropogenic landscapes. Environ. Res. Lett. 11, 035014. https://doi.org/10.1088/1748-9326/11/3/035014.

Vengosh, A., 2003. Salinization and Saline Environments. Ch. 9.09 in Sherwood Lollar B. (Ed.) Treatise on Geochemistry, 9: 333-365. ISBN 0-08-043751-6. Elsevier, https://ui.adsabs.harvard.edu/link_gateway/2003TrGeo...9..333V/ doi:10.1016/B0-08-043751-6/09051-4.

Verstraete, M.M., Scholes, R.J., Smith, M.S., 2009. Climate and desertification: looking at an old problem through new lenses. Front. Ecol. Envir. 7, 421–428. https://doi.org/10.1890/080119.

WHO (World Health Organization), 2022. Guidelines for drinking-water quality: Fourth edition incorporating the first and second addenda, ISBN 978-92-4-004506-4 Licence: CC BY-NC-SA 3.0 IGO, https://www.who.int/publications/i/item/9789240045064.

Zak, D., Hupfer, M., Cabezas, A., Jurasinski, G., Audet, J., Kleeberg, A., McInnes, R., Kristiansen, M.S., Petersen, R.J., Liu, H., Goldhammer, T., 2021. Sulphate in freshwater ecosystems: a review of sources, biogeochemical cycles, ecotoxicological effects and bioremediation. Earth Sci. Rev. 212, 103446. https://doi.org/10.1016/j.earscirev.2020.103446.